



HAL
open science

Protein kinase R induced by type I interferons is a main regulator of reactive microglia in Zika virus infection

Violaine Bortolin, Zeyni Mansuroglu, Laurine Conquet, Gaetano Calcagno, Fanny Lambert, Jose Pablo Marin-Obando, Helena Segrt, Mary Savino, Reyene Menidjel, Sylvie Souès, et al.

► To cite this version:

Violaine Bortolin, Zeyni Mansuroglu, Laurine Conquet, Gaetano Calcagno, Fanny Lambert, et al.. Protein kinase R induced by type I interferons is a main regulator of reactive microglia in Zika virus infection. *Glia*, In press, DOI: 10.1002/glia.24619 . hal-04798761

HAL Id: hal-04798761

<https://hal.science/hal-04798761v1>

Submitted on 3 Dec 2024

HAL is a multi-disciplinary open access archive for the deposit and dissemination of scientific research documents, whether they are published or not. The documents may come from teaching and research institutions in France or abroad, or from public or private research centers.

L'archive ouverte pluridisciplinaire **HAL**, est destinée au dépôt et à la diffusion de documents scientifiques de niveau recherche, publiés ou non, émanant des établissements d'enseignement et de recherche français ou étrangers, des laboratoires publics ou privés.



Distributed under a Creative Commons Attribution - NonCommercial - NoDerivatives 4.0 International License

RESEARCH ARTICLE

Protein kinase R induced by type I interferons is a main regulator of reactive microglia in Zika virus infection

Violaine Bortolin¹ | Zeyni Mansuroglu¹ | Laurine Conquet² | Gaetano Calcagno² | Fanny Lambert¹ | Jose Pablo Marin-Obando¹ | Helena Segrt³ | Mary Savino¹ | Reyene Menidjel¹ | Sylvie Souès¹ | Luc Buée³ | Florence Niedergang¹ | Marie-Christine Galas³ | Xavier Montagutelli²  | Eliette Bonnefoy¹ 

¹CNRS, Inserm, Institut Cochin, Université Paris Cité, Paris, France

²Institut Pasteur, Université Paris Cité, Mouse Genetics Laboratory, Paris, France

³Inserm, CHU Lille, CNRS, LiNCog–Lille Neuroscience & Cognition, University of Lille, Lille, France

Correspondence

Eliette Bonnefoy, CNRS, Inserm, Institut Cochin, Université Paris Cité, F-75014 Paris, France.

Email: eliette.bonnefoy@inserm.fr

Funding information

Agence Nationale de la Recherche, Grant/Award Numbers: ANR-10-LABX-62-IBEID, ANR-20-CE16-0017; Institut National de la Santé et de la Recherche Médicale; Conseil National de la Recherche Scientifique; Université Paris Cité

Abstract

Microglial cells are the phagocytic cells of the brain that under physiological conditions participate in brain homeostasis and surveillance. Under pathogenic states, microglia undergoes strong morphological and transcriptional changes potentially leading to sustained neuroinflammation, brain damage, and cognitive disorders. Postnatal and adult Zika virus (ZIKV) brain infection is characterized by the induction of reactive microglia associated with brain inflammation, synapse loss and neuropathogenesis. Contrary to neurons, microglial cells are not infected by ZIKV thus raising the question of the mechanism governing ZIKV-induced microglia's reactivity. In this work, we have questioned the role of exogenous, neuronal type I interferons (IFNs-I) in regulating ZIKV-induced microglia's reactivity. Primary cultured microglial cells were either treated with conditioned media from ZIKV-infected mature neurons or co-cultured with ZIKV-infected neurons. Using either an antibody directed against the IFNAR receptor that neutralizes the IFNs-I response or *Ifnar*^{-/-} microglial cells, we demonstrate that IFNs-I produced by ZIKV-infected neurons are the main regulators of the phagocytic capacity and the pro-inflammatory gene expression profile of reactive, non-infected microglial cells. We identify protein kinase R (PKR), whose expression is activated by IFNs-I, as a major regulator of the phagocytic capacity, pro-inflammatory response, and morphological changes of microglia induced by IFNs-I while up-regulating STAT1 phosphorylation and IRF1 expression. Results obtained herein in vitro with primary cultured cells and in vivo in ZIKV-infected adult immunocompetent mice, unravel a role for IFNs-I and PKR in directly regulating microglia's reactivity that could be at work in other infectious and non-infectious brain pathologies.

KEYWORDS

collaborative cross mice, inflammation, kinase PKR, microglia, phagocytosis, zika virus, type I interferon

This is an open access article under the terms of the [Creative Commons Attribution-NonCommercial-NoDerivs](https://creativecommons.org/licenses/by-nc-nd/4.0/) License, which permits use and distribution in any medium, provided the original work is properly cited, the use is non-commercial and no modifications or adaptations are made.

© 2024 The Author(s). GLIA published by Wiley Periodicals LLC.

1 | INTRODUCTION

Microglial cells are the innate immune, phagocytic cells of the central nervous system (CNS) that arise from primitive myeloid precursor cells, reaching the brain rudiment early during embryogenesis. They are highly plastic cells that dynamically respond to local environmental inputs persisting in adulthood as long-lived cells maintained by slow local self-renewal (Arutyunov & Klein, 2023; Chhatbar & Prinz, 2021; Paolicelli et al., 2022).

Under physiological conditions, microglia is involved in brain homeostasis and surveillance maintaining the CNS health and influencing learning and memory (Borst et al., 2021; Garaschuk & Verkhratsky, 2019; Ransohoff & El Khoury, 2015). They are characterized by a ramified morphology with a small cell body and multiple long, thin ramified processes that are constantly moving, surveying their proximal environment (Savage et al., 2019). They shape neuronal networks during development and adulthood eliminating inactive synapses through complement 3 (C3)-dependent phagocytosis (Schafer et al., 2012; Stevens et al., 2007; Wang et al., 2020). They secrete neurotrophic factors (Borst et al., 2021), eliminate cellular debris (Neumann et al., 2009), and protect the CNS against pathological inputs (Borst et al., 2021). In the adult “healthy” brain, microglial cells display little transcriptional heterogeneity except for variations related to the brain region (Grabert et al., 2016; Lopes et al., 2022), the age (Grabert et al., 2016; Lopes et al., 2022; Olah et al., 2018; Sala Frigerio et al., 2019) and the sex (Sala Frigerio et al., 2019; Villa et al., 2018).

In response to local CNS signals associated with different pathogenic states of the CNS, microglial cells undergo strong morphological and transcriptional changes adopting a hypertrophic morphology with a large cell body and short processes (Savage et al., 2019; Schwabenland et al., 2021). They interact with neurons and synapses, potentially leading to the pathological destruction of functional synapses in link with a sustained neuroinflammatory response and the development of cognitive disorders (Butler et al., 2021; Hong et al., 2016; Roy et al., 2020; Vasek et al., 2016). Compared with homeostatic microglia, microglia associated with neurological pathologies are highly heterogeneous (Paolicelli et al., 2022) in such a way that reactive microglial cells are classified into varying subsets displaying among other diverse transcriptional signatures (e.g. disease associated microglia, DAM; activated response microglia, ARM; interferon-responsive microglia, IRM; proliferative associated microglia, PAM) (Borst et al., 2021; Butovsky & Weiner, 2018; Chhatbar & Prinz, 2021; Lopes et al., 2022; Olah et al., 2020; Paolicelli et al., 2022; Sala Frigerio et al., 2019). Microglial subsets displaying a type I interferon (IFN-I) response signature (IRM) have been found associated with the development of Alzheimer's disease (AD) in AD murine models (Chen & Colonna, 2021; Ising et al., 2019; Mathys et al., 2017; Sala Frigerio et al., 2019) and post-mortem human samples (Chen & Colonna, 2021; Olah et al., 2020; Taylor et al., 2014) as well as in association with traumatic brain injury (Todd et al., 2023) and aging (Deczkowska et al., 2017; Lopes et al., 2022; Olah et al., 2018; Sala Frigerio et al., 2019) raising the question of the role of type I interferons (IFNs-I) on microglia's reactivity.

The IFN-I response constitutes the main innate antiviral response designed to inhibit viral replication and propagation. It is triggered by the recognition of cytoplasmic nucleic acids, mostly of viral origin, by pattern-recognition receptors (PRRs) (Jensen & Thomsen, 2012) leading to the rapid transient up-regulation of the expression of the *Ifnb1* gene coding for IFN beta (IFNB). After binding to its receptor IFNAR present on the surface of most cell types (including neurons), IFNB activates the phosphorylation of transcription factors STAT1 and 2 further inducing the expression of a large set of interferon stimulated genes (ISGs) including the genes coding for IFNs alpha (IFNsA) that amplify the response (Schneider et al., 2014). While the IFN-I response is essentially an antiviral system, it can also be triggered by endogenous, cytoplasmic host DNAs and RNAs (Crow & Stetson, 2022) promoting brain inflammation and neurological disorders (Baruch et al., 2014; Crow & Manel, 2015; Crow & Stetson, 2022; Hofer & Campbell, 2013).

In this work we have analyzed the effect of IFNs-I secreted by ZIKA virus (ZIKV)-infected neurons as well as of recombinant IFNB on microglia's C3-dependent phagocytosis and pro-inflammatory response while questioning the role on this effect of the kinase PKR, encoded by a main ISG (Schneider et al., 2014). ZIKV is a human, emerging, neurotropic, mosquito-borne flavivirus (Javed et al., 2018) for which there is evidence in humans (Acosta-Ampudia et al., 2018; da Silva et al., 2017; Lannuzel et al., 2019), macaques (Hsu et al., 2022; Raper et al., 2020), and mice (de Oliveira Souza et al., 2018; Figueiredo et al., 2019) that delayed neuropathies of the CNS, associated with cognitive disorders, can develop following neonatal and adult infections. Reactive microglia is a major trait of ZIKV brain infection yet, in adult human and mice brain, ZIKV infects neurons but not microglial cells (Figueiredo et al., 2019; Hayashida et al., 2019; Manet et al., 2020; Manet et al., 2022). The capacity of IFNs-I and PKR to affect microglia's reactivity was analyzed at the molecular and cellular level in vitro, with mature primary cultured microglia (PCM) and neurons (PCNs) (alone or combined) and in vivo, following intracranial (IC) ZIKV infection of immunocompetent mice that, contrary to immuno-comprised mice often used in the context of ZIKV infection (Christian et al., 2019), have an inducible antiviral IFN-I response.

2 | MATERIALS AND METHODS

Virus: The FG15 Asian ZIKV strain, isolated from a patient during a ZIKV outbreak in French Guiana in December 2015, was obtained from the Virology Laboratory of the Institut Pasteur of French Guiana. Viral stocks were prepared from the supernatant of infected C6/36 cells, clarified by centrifugation and titrated on Vero cells (ATCC, CRL-1586) by a focus-forming assay (FFA). Stocks were kept at -80°C . All experiments with ZIKV were carried out in biosafety level three facilities.

Mice: C57BL/6J (B6) mice (purchased from Janvier Labs France), B6-*Ifnar* KO mice (from Institut Pasteur animal facility, France), and Collaborative Cross CC071 mice (purchased from the Systems

Genetics Core Facility, University of North Carolina and bred at the Institut Pasteur) were maintained under specific-pathogen-free conditions with a 14-h light and 10-h dark cycle and ad libitum food and water. In all experiments, mice were killed by cervical dislocation. All experimental protocols were approved by the Institut Pasteur Ethics Committee (dap190107) and authorized by the French Ministry of Research (#19469), in compliance with French and European regulations.

Antibodies: Primary and secondary antibodies used for immunofluorescence and Western blot are listed in Table 1.

Primary culture of microglia: Primary cultured microglial cells (PCMCs) were prepared from pools of cortices from 0- or 1-day-old newborn B6 mice ($n = 12$ newborns per culture) either wild type or *Ifnar* KO. After decapitation, hemispheres were dissected and stripped of meninges, olfactory bulbs, and cerebellum. Cortices were incubated at 37°C with 0.25% trypsin (Gibco, 25200-056) for 15 min and with 0.6 mg/mL final concentration of DNase I (Sigma, 11284932001) for 5 min and then mechanically dissociated with a pipette. After

dissociation, glial cells were plated into poly-L-ornithine- (Sigma, P3655) coated cell culture dishes containing glial culture medium: DMEM (Gibco, 31885) supplemented with 10% heat-inactivated fetal bovine serum (FBS, Gibco), 0.5% penicillin-streptomycin (Gibco, 15140-148) and 1% L-Glutamine (Gibco, 25030-024). Cells were maintained in incubators at 37°C 5% CO₂ and medium was replaced at 1 and 3 DIV (days in vitro). Microglia were detached from the astrocytic layer after 13 DIV by gentle shaking and plated in 12-well plates with 600,000 cells/well for RNA extraction and Western blot, in 24-well plates containing coverslips with 100,000 cells/well for immunofluorescence and phagocytosis. The absence of astrocytes was confirmed by immunofluorescence and RT-qPCR (Figure S1a,b). Cells were maintained in glial culture medium at 37°C and 5% CO₂. One day after plating, cells were either treated with conditioned media (CMs) from non- or ZIKV-infected primary cultured neurons (PCNs), treated with indicated amounts of murine recombinant IFNB (8234 MB, Bio-Techne) at final concentrations ranging from 50 to 5000 U/mL with 1000 U/mL = 1 ng/mL or infected. For treatments

TABLE 1 Antibodies.

| Primary antibodies | Species | Source | Reference | Figure |
|---------------------------|------------|------------------------|-----------------|---------------------------|
| Anti-MAP2 | Mouse | Sigma | M4403-50UL | Figure 3a-c |
| Anti-MAP2 | Goat | Bio-Techne | NBP3-05552-50UL | Figure 3d |
| Anti-ZIKV NS2B | Rabbit | Euromedex | GTX133308 | Figures 3a-c, 5a, and 6f |
| Anti-Iba1 | Rabbit | Wako | 019-19,741 | Figures 3d, 7a,b, and S1a |
| Anti-Iba1 | Goat | Sobodia | 011-27,991 | Figure 3c |
| Anti-Iba1 | Goat | Abcam | Ab5076 | Figures 5a and 6f |
| Anti-NeuN | Guinea pig | Merck | ABN90 | Figures 5a and 6f |
| Anti-GAPDH | Mouse | Cell Signaling | 97,166 | Figure 9a-d,g-j |
| Anti-BActin HRP | Mouse | Santa Cruz | sc-47,778 | Figure 9e,f |
| Anti-STAT1 | Mouse | BD | 610,115 | Figure 9a-d,i |
| Anti-phSTAT1 | Rabbit | Cell Signaling | 91,675 | Figure 9a-d,i |
| Anti-IkB | Mouse | Santa Cruz | sc-56,710 | Figure 9e-h |
| Anti-phIkB | Mouse | Cell Signaling | 9246 | Figure 9e-h |
| Anti-IRF3 | Mouse | Cell Signaling | 4302S | Figure 9a |
| Anti-phIRF3 | Mouse | Cell Signaling | 4947S | Figure 9a |
| Anti-IRF1 | Rabbit | Cell Signaling | 8478S | Figure 9j |
| Secondary antibodies | Species | Source | Reference | Figure |
| Anti-mouse Alexa 647 | Chicken | Invitrogen | A-21463 | Figure 3a,b |
| Anti-mouse Alexa 488 | Chicken | Invitrogen | A-21200 | Figure 3c |
| Anti-rabbit Cy3 | Donkey | Jackson ImmunoResearch | 711-166-152 | Figure 3a-d |
| Anti-goat Alexa 647 | Chicken | Invitrogen | A-21469 | Figure 3c,d |
| Anti-mouse HRP | Donkey | Jackson ImmunoResearch | 715-035-151 | Figure 9a-j |
| Anti-rabbit HRP | Donkey | Jackson ImmunoResearch | 711-035-152 | Figure 9a-d,i,j |
| Anti-rabbit Alexa 488 | Goat | Thermo Fisher | A11008 | Figures 5a and 6f |
| Anti-goat Alexa 568 | Donkey | Thermo Fisher | A11057 | Figures 5a and 6f |
| Anti-guinea pig Alexa 647 | Goat | Thermo Fisher | A21450 | Figures 5a and 6f |

with CMs and ZIKV, the whole medium was removed and replaced with 0.5 mL of either glial culture medium, CMs collected from non- or ZIKV-infected PCNs or medium containing ZIKV viral particles. Recombinant IFNB or Newcastle Disease Virus (NDV) diluted in 100 μ L of medium were added directly in the culture medium. When indicated, MAR1-5A3 anti-IFNAR antibody (ThermoFisher, 15820839) was added overnight at 2.6 μ g/mL final concentration. The inhibitor of PKR (iPKR) C16 (Merck, 527450) at a 50 μ M final concentration (unless indicated otherwise) or the corresponding volume of DMSO was added directly in the culture medium for 1 h before treatment or infection as described by Pham et al. (2016). Following incubation with C16, the inhibitor was removed and cells further treated as indicated.

Complemented C3 opsonization of sheep red blood cells and phagocytosis: Sheep blood was obtained from Rockland Clinisciences (R311-0050) and purified in Alsevers solution. Purified sheep red blood cells (SRBCs) were washed two times with PBS-0.1% bovine serum albumin and incubated with anti-SRBC rabbit IgM (MyBioSource, 0544-MB5524107) for 30 min at room temperature (RT) with rotation. After centrifugation (4 min at 4000 rpm), SRBC-IgM were washed with PBS and re-suspended in glial culture medium without serum. Complement C3 present in C5-deficient human serum (Sigma, C1163) was added to the resuspended SRBC-IgM to a 10% (volume *per volume*) final concentration and incubated for 20 min at 37°C. After centrifugation (4 min at 4000 rpm), SRBC-IgM opsonized with C3 (C3-SRBCs) were re-suspended in pre-warmed glial culture medium without serum. For phagocytosis of C3-SRBCs by PCMCs, 0.5 mL of glial medium containing C3-SRBCs were added to PCMCs cultured in 24-well plates containing coverslips to a final ratio of 15 C3-SRBCs *per* microglial cell. After adding C3-SRBCs, culture plates were centrifuged for 2 min at 4°C at 1500 rpm and then either placed on ice and immediately fixed (T0) or fixed after 15 min of incubation at 37°C (T15), in order to allow for phagocytosis to take place before fixation. Cells were fixed with 4% formaldehyde for 15 min at RT. C3-SRBCs were labeled using an F(ab)₂ anti-rabbit antibodies coupled to Cy3 (Jackson ImmunoResearch, 715-546150) that recognizes the IgM bound to SRBCs.

Primary neuronal culture: Primary cortical neurons were prepared from individual fetuses from two or more genetically identical B6 females at day 15.5 and 16.5 of gestation. Cortexes from 6 to 8 fetuses/female were carefully dissected out, incubated for 15 min with Trypsin (Sigma, T6763) and DNase I (Sigma, 11284932001) at 1 and 0.5 mg/mL final concentration respectively and mechanically dissociated by triturating with a polished Pasteur pipette. Each embryo was dissected individually and cells from the different fetuses were mixed before plating. Neurons were maintained in Neurobasal medium supplemented with B27 supplement (Gibco, 17504-044), L-glutamine (Gibco, 25030-024) and antibiotic/antimycotic (Gibco, 15240-096). Tissue culture plate wells and coverslips for immunofluorescence microscopy were coated with poly-D-lysine 0.1 mg/mL (Sigma, P7280) and laminin 20 μ g/mL (Sigma, L2020) final concentrations. For RNA extraction, cells were plated in 6-well plates with 600,000 cells/well. For immunofluorescence and WB, cells were plated in 12-well plates

with 120,000 and 250,000 cells/well respectively. Cells were maintained at 37°C and 5% CO₂. The total volume of culture medium was changed at 1 DIV and one third of the culture medium was changed at 8 DIV. Primary cultured neurons (PCNs) were infected at a multiplicity of infection (MOI) = 5 at 11 DIV. For ZIKV infection, 1 mL of medium was removed and replaced with 1 mL of medium containing the virus. Two hours after infection, the inoculum was removed and new culture medium (2/3 fresh and 1/3 old) was added. For NDV infection, NDV diluted in 100 μ L of medium was added directly in the culture medium. The IPKR C16 (Merck, 527450) at a 50 μ M final concentration or the corresponding volume of DMSO was added directly in the culture medium for 1 h before treatment or infection.

Primary co-cultures of neurons and microglia: Neurons and microglia cultured as previously indicated were mixed together at a neuron: microglia ratio of 5:1. For this, microglial cells were detached from the astrocytic layer by gentle shaking at 10 DIV. After washing with PBS, PCMCs were resuspended in neurobasal medium and added to the 8 DIV-old primary neuronal culture. Three to four days after adding microglial cells, co-cultures were infected as previously described for ZIKV-infection of PCNs.

Mouse ZIKV intracerebral (IC) infection: All infection experiments were performed in a biosafety level 3 animal facility as described previously (Manet et al., 2020). After being anesthetized by intraperitoneal (IP) injection of Ketamine 70 mg/kg and Xylazine 5 mg/kg, groups of 5- to 6-week-old mice were inoculated by IC injection. Mice received either 10⁵ foci forming units (FFUs) of ZIKV FG15 in NaCl or NaCl alone in a volume of 10 μ L. Survival and clinical signs were monitored daily for 6 days, and the mice were euthanized for brain collection. When indicated, 20 μ g of the PKR inhibitor C16 (Merck, 527450) were administered 45 min before and 3 days after infection. A 5 mg/mL stock of C16 in 100% DMSO was diluted 1:25 in NaCl and 100 μ L were injected intraperitoneally (IP). Control group received 100 μ L of 4% DMSO in PBS.

RT-qPCR: Total RNA from primary cultured and co-cultured neurons and microglia was extracted using the RNeasy Plus kit (Qiagen). Brain tissue samples were homogenized at 4°C in 1 mL of Trizol reagent (Life technologies), using ceramic beads and an automated homogenizer (PreCellys). RNA was reversely transcribed using high capacity cDNA Reverse Transcription Kit (Applied Biosystems) according to the manufacturers' recommendations using random primers. qPCR was performed using SENSIFAST SYBR NO-ROX MIX (Bio-TechnoFix) reagents at: 95°C 2 min, then 40 cycles at 95°C 5 s, 60°C 10 s, 72°C 15 s, followed by a dissociation step. Relative quantification of mRNA expression was calculated by the $\Delta\Delta C_T$ method using as reference genes: *Rplp0* for PCNs and PCMCs and *Hrpt1* for brain extracts. Sequences (5'-3') of primers used for qPCR analysis are listed in Table 2.

Immunofluorescence, immunohistochemistry, and image analysis:

(i) PCNs and PCMCs: Primary neurons and microglia cultured alone or combined were fixed with 4% formaldehyde in PBS at RT for 15 min and permeabilized with 0.5% Triton X-100 in PBS at RT for 10 min for microglia and 30 min for neurons and co-cultures. The cells were incubated for 1 h at RT with the corresponding primary antibodies (listed in Table 1) diluted in PBS-5% bovine serum albumin.

TABLE 2 Oligonucleotides.

| RNA amplified | Forward oligo | Reverse oligo |
|---------------|-------------------------|--------------------------|
| Rplp0 | cactggtctaggaccgagaag | ggtgcctctggagatcttcg |
| Hprt1 | tcctcctagaccgctttt | cctggttcatcatcgtaatc |
| ZIKV RNA | ccgctgcccaacacaag | ccactaacgttctttgcagacat |
| Ifnb1 | cagctccaagaaggacgaac | ggcagtgtaactctctgcat |
| Irf7 | cagcgagtgtctgttgagac | aagttctacaccttatgctg |
| Irf1 | actgaatcgggatgagacc | tgctttgatcggcctgtgt |
| Ifn4 | tgatgactactactggtcagc | gatctcttagcacaaggatggc |
| Isg15 | catctatgaggtctttctgacgc | ttaggccatactccccagc |
| Eif2ak2 | ttcacacgtcttcacggagt | atgtctcaggtcggctcttg |
| Usp18 | cgtgttggtttacacaacat | gaggcactgttatctcttc |
| Cxcl10 | gacggtccgctgcaactg | gcttccctatggccctcatt |
| Il6 | agttgccttctgggactga | tccacgatttccagagaac |
| Nos2 | gccaccaacaatggcaaca | cgtaccggatgagctgtgaatt |
| Tnf | ccctcacactcagatcatcttct | gctacgacgtgggctacag |
| Ccl5 | gtgctccaactctgacgtgtgt | acttcttctctgggttgccacaca |
| Ccl2 | ggtccctgtcatctctctg | gttaactgcatctggctgag |
| Il1b | tgccaccctttgacagtgatg | aaggtccacggaaagacac |
| C4 | ggcagcacaatcagtgtaaa | tcattggcatcccatcgtatt |
| C3 | ggaagatccgagccttttac | ccacaccatcctaatcactac |
| C1qa | tctcagccattcggcagaac | taacacctggaagagccctt |
| Aif1 | cagggatttcagggaggaa | gtagctgaactctctctcg |
| Bdnf | gccttcatgcaaccgaagta | tgagtctccaggacagcaaa |
| Mef2c | agatctgacatccggtgacg | tcttgttcaggttaccaggtg |
| Apoe | agaccctggagcctaaggac | agagccttcatcttcgcaat |
| Clec7a | atggttctgggagatggat | cctggggagctgtattctg |
| Cx3cr1 | tgagtactggcacttctctg | cgaggaccaccaacagattt |
| Ifnb | aactggcaaaaggatggt | gacctcaacttgcaaac |
| Gfap | acaccagcacttcccttctt | tctgctcatcttctcttcc |
| Cd11b | ccttcatcaacaacagagtggt | cgaggtgctctaaaccaagc |
| NDV RNA | agtgatgtgctcggaccttc | cctgaggagaggcatttgcta |

After washing with PBS, the cells were next incubated for 45 min at RT with the corresponding secondary antibodies (listed in Table 1), Hoechst (Invitrogen, 33342) and when indicated, phalloidin-Alexa 488 (Molecular Probes, A12379) or -Alexa 633 (Molecular Probes, A22284). For phagocytosis, samples were analyzed using an inverted wide-field microscope (Leica DMI6000) with a 100x (oil) objective and an ORCA flash 4 camera (Hamamatsu). Z-series of images were taken at 0.25 μ m increments. For the determination of phagocytosis and association indexes, images were acquired blindly, only looking at DAPI (nucleus) staining. In Figure 1, samples were analyzed with an inverted microscope (Leica DMI6000) equipped with a confocal Spinning Disc scanning head (Spinning Disc Yokogawa CSU-X1M1). This system is equipped with a 63 \times lens, 1.4-numerical-aperture oil immersion lens (Plan APO) and motorized platine XY (Märzhäuser Wetzlar SCAN IM 127–83). Images were captured in the z-axis corresponding to the optical axis of the microscope at 0.30 μ m intervals.

MetaMorph 7.7.5 (Molecular devices) imaging software was used for image capture. The images were analyzed using the Image J software (National Institute of Health).

(ii) Brains slices: Immunofluorescence was performed at the confocal microscopy platform IMPRT (Institut de Médecine Prédictive et de Recherche Thérapeutique, Lille) as described previously (Violet et al., 2015). Images of hippocampal sections from CC071 mice were acquired using LSM 710 confocal laser-scanning microscope (Carl Zeiss). The confocal microscope was equipped with a 488-nm Argon laser, 561-nm diode-pumped solid-state laser, and a 405-nm ultraviolet laser. The images were acquired using an oil 63 \times Plan-APOCHROMAT objective (1.4 NA). All recordings were performed using the appropriate sampling frequency (16 bits, 1024–1024 images, and a line average of 4). Immunohistochemistry was performed at the HistIM platform of Institut Cochin. Slides were incubated for 15 min at 95°C in a solution of deparaffinization and antigen retrieval at pH 6 before incubation 20 min at RT with the primary antibodies. Detection was performed using a Leica BOND Polymer Refine Detection System DS9800. Sections were lightly counterstained with hematoxylin, then dehydrated and cleared in graded alcohol and Ottix plus (MM-France), and finally covered with glass slips. Images were acquired using a Lamina slide scanner (Perkin Elmer) and analyzed using the QuPath software.

ImmunoFISH: For immunoFISH (Figure 3b), cells were treated for immunofluorescence before in situ RNA hybridization. Following immunofluorescence, cells were post-fixed for 5 min at RT with 4% paraformaldehyde in PBS, washed 2 times for 5 min in PBS and with Stellaris RNA FISH Wash Buffer A (Biosearch Technologies, SMF-WA1-600) containing 10% formamide for 5 min. Coverslips were hybridized with Stellaris RNA FISH Hybridization Buffer (Biosearch Technologies, SMF-HB1-10) containing 10% formamide and 1% of ZIKV positive strand probe (Biosearch Technologies, SS858758-01-47). Hybridization was performed on slides overnight at 37°C. After hybridization, coverslips were washed with Stellaris RNA FISH Wash Buffer A 10% formamide for 30 min at 37°C, followed by incubation with Hoechst (Invitrogen, 33,342) diluted in PBS 1X for 30 min at RT and washed with Stellaris RNA FISH Wash Buffer B (Biosearch Technologies, SMF-WB1-200).

Western blot: Total protein extracts from PCMCs were collected in 2 \times Laemmli buffer for a final concentration of approximately 1.5 \times . After heating, protein extracts were loaded in sodium dodecyl sulfate Bolt 4%–12% Bis-Tris polyacrylamide precast non-reducing gels (Life technologies). Loaded proteins were transferred on PolyVinylidene diFluoride (PVDF) membrane. Membranes were incubated overnight at 4°C with primary antibodies (listed in Table 1), washed with TBS-T (Tris Base Sodium Tween 0.1%) and incubated with the corresponding secondary antibodies (listed in Table 1) for 1 h at RT. Fusion FX Vilber Lourmat was used for chemiluminescent protein detection. Relative quantification of proteins was carried out using Image J software.

Statistics: Data were analyzed using Prism version 9.4 (GraphPad Software). The statistical analysis used and the number, *n*, of independent experiments or mice is specified in the corresponding figure legends. When the data was analyzed using a paired *t*-test, independent paired experiments were represented in different colors.

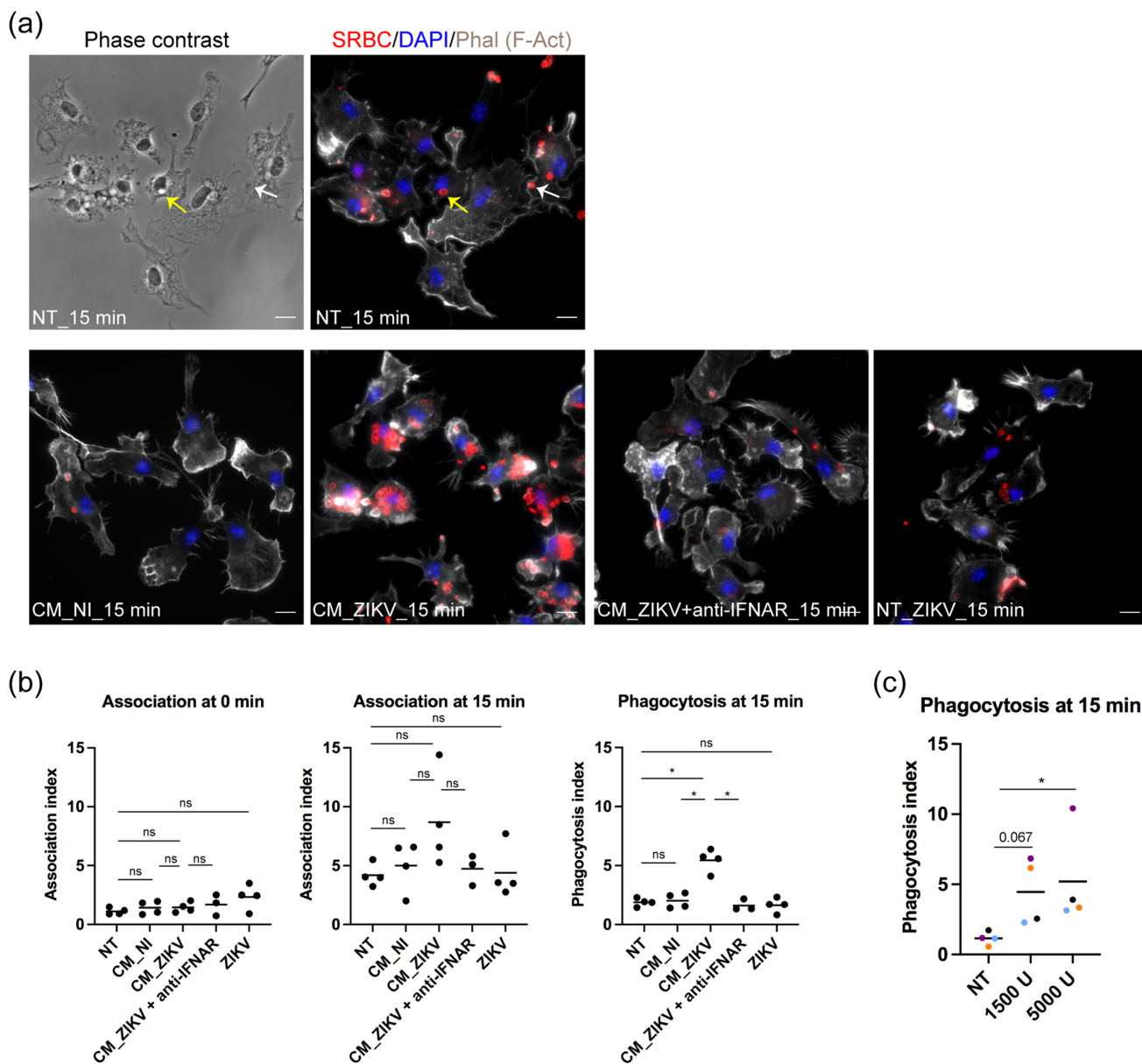


FIGURE 1 Exogenous IFNs-I increase the phagocytic capacity of non-infected microglia. (a, b) Four independent primary cultures of microglial cells were incubated with conditioned media collected from three independent non- or ZIKV-infected PCNs at 64 h post-infection (p.i) for 6 h before being incubated with sheep red blood cells opsonized with complement C3 (C3-SRBC). After 15 min incubation with C3-SRBC, PCMCs were fixed and analyzed in a wide field microscope. (a) Phase contrast and immunofluorescence analysis with filamentous Actin (F-Act) labeled with phalloidin, SRBCs labeled with anti-sheep antibody and DNA labeled with DAPI. White arrow indicates an external (bound but not phagocytosed) SRBCs and yellow arrow indicates an internal (phagocytosed) SRBCs. Scale bars = 10 μm. (b) The association (external + internal SRBCs/cell) and phagocytosis (internal SRBCs/cell) indexes were determined after counting the external and internal SRBCs from a minimum of 35 cells/independent experiment. Dot plots show means with one dot for each independent experiment. Significance was assessed by one-way ANOVA Tukey's multiple comparison test. p -value < 0.05 (*) and ns = not significant. (c) PCMCs were incubated with increasing amounts of recombinant IFNβ for 6 h before being incubated with C3-SRBCs. After 15 min incubation with C3-SRBCs, PCMCs were fixed and analyzed in a wide field microscope as in (a) and the phagocytosis index was determined as in (b). Dot plots show means with one dot for each independent experiment represented in a different color. Significance was assessed by ratio paired t -test. p -value < 0.05 (*) and ns = not significant; p -value near significance is indicated.

3 | RESULTS

3.1 | Exogenous IFNs-I activate the phagocytic capacity and the pro-inflammatory response of PCMCs

In order to test the effect of IFNs-I secreted by ZIKV-infected PCNs on the phagocytic capacity of PCMCs, C3-SRBCs were added to

microglial cells either non-treated (NT) or previously treated for 6 h with conditioned media collected from non- (CM_NI) or ZIKV-infected (CM_ZIKV) PCNs in the presence or absence of an antibody directed against the IFNs-I receptor (anti-IFNAR) that neutralizes IFNs-I signaling (Sheehan et al., 2006). In parallel, C3-SRBCs were added to microglial cells previously incubated for 6 h with the same amount of ZIKV present in CM_ZIKV as determined by titration (NT_ZIKV). After

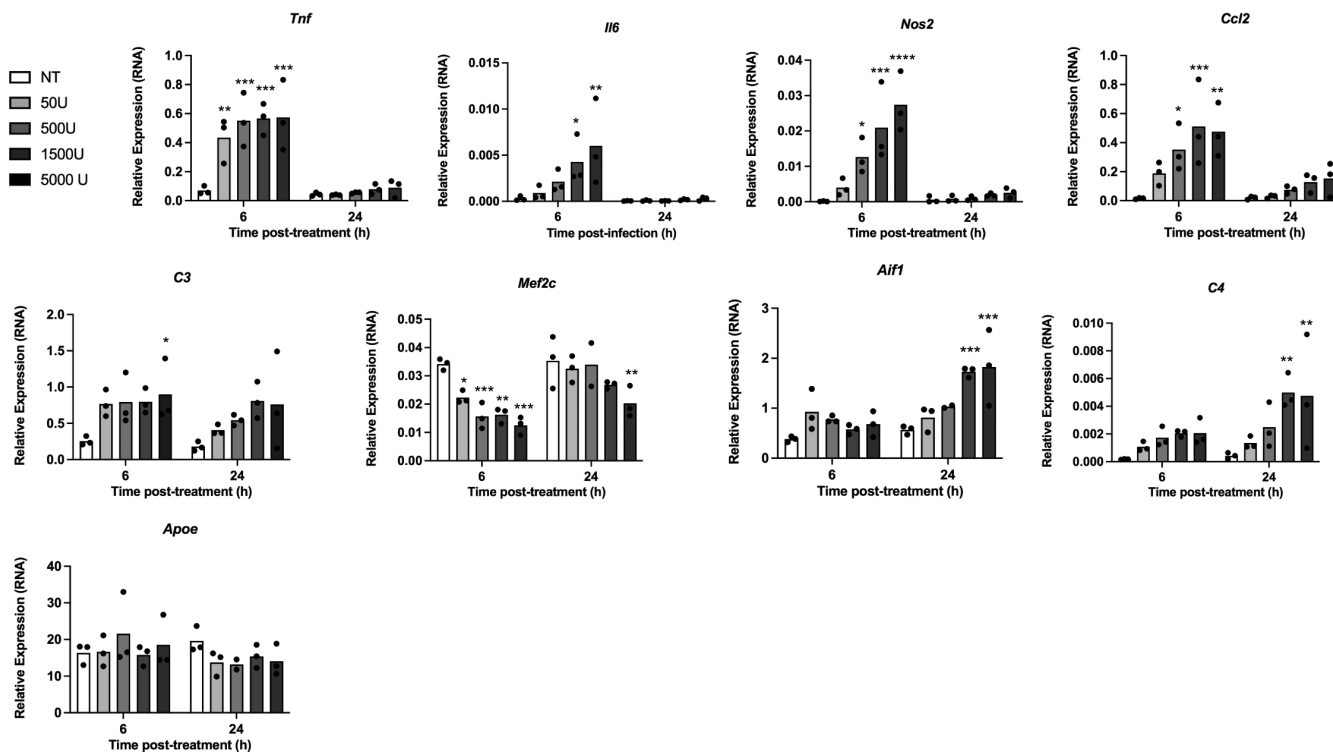


FIGURE 2 Treatment with recombinant IFNB activates the pro-inflammatory gene expression profile of non-infected microglia. Primary cultured microglial cells (PCMCs) were treated with increasing amounts of recombinant IFNB for 6 and 24 h before collection of RNAs. Levels of RNA expression were determined by RT-qPCR with respect to *Rplp0* used as reference gene. Bars represent means with symbols corresponding to each independent experiment. Significance was assessed by two-way ANOVA Dunnett's multiple comparison test compared with the corresponding NT conditions. p -value <0.0001 (****), <0.001 (***), <0.01 (**), <0.05 (*), and ns = not significant.

adding C3-SRBCs, microglial cells were either immediately fixed (T0) or further incubated for 15 min at 37°C before fixation (T15). Phase contrast and fluorescence microscopy images (Figure 1a) were used in order to determine the external (bound but not yet phagocytosed) and the internal (phagocytosed) C3-SRBCs as indicated by a white and yellow arrow respectively in Figure 1a (NT_15 min panels). The corresponding indexes of association (internal and external C3-SRBCs per cell) and of phagocytosis (internal C3-SRBCs per cell) were determined (Figures 1b and S1a). As expected, association but not phagocytosis was observed at T0 (Figures 1b and S1a) with no significant variations observed for the association index at T0 among the different conditions analyzed (Figure 1b). Both, the association and phagocytosis indexes increased at T15 (Figure 1b) with respect to T0 (Figures 1b and S1c). The incubation of PCMCs with CM_ZIKV strongly increased the amount of C3-SRBCs phagocytosed at T15 by microglial cells with respect to microglial cells NT, treated with CM_NI or ZIKV alone (ZIKV) (Figure 1a,b). The increase of the phagocytic capacity of microglial cells induced by CM_ZIKV was abolished in the presence of the anti-IFNAR antibody (Figure 1a,b), indicating that IFNs-I present in CM_ZIKV were the main factors responsible for the activation of phagocytosis. No significant effect was observed in the presence of ZIKV alone, ruling out a direct effect of the virus on microglial cells. No ZIKV RNA was detected after treatment of microglial cells with CM_ZIKV in contrast to ZIKV-infected neurons from which CMs were collected (Figure S1d), in agreement with the inability of ZIKV to infect microglial cells.

The capacity of exogenous IFNs-I to activate C3-dependent phagocytosis by microglial cells was further investigated by incubating PCMCs with recombinant IFNB (reclFNB) for 6 h prior to adding C3-SRBCs. After 6 h of incubation with reclFNB, the phagocytic capacity of microglial cells was significantly increased (Figure 1c) reaching a phagocytosis index similar to the one induced by CM_ZIKV (Figure 1b).

The response of microglial cells to reclFNB was further analyzed with respect to their capacity to mount a pro-inflammatory response (Figure 2). As previously observed following treatment of PCMCs with CM_ZIKV (Manet et al., 2022, Figure 5), a significant or near significant induction of the expression of pro-inflammatory genes such as *Tnf*, *Il6*, *Nos2*, and *Ccl2* (Figure 2) and of the *C3* gene coding for complement factor C3 was rapidly observed after 6 h treatment of PCMCs in correlation with the amount of reclFNB, alongside with a significant inhibition of the expression of the *Mef2c* gene that codes for a negative regulator of the microglia inflammatory response (Deczkowska et al., 2017). A late activator effect was observed after 24 h of treatment for the expression of the *Aif1* gene coding for IBA1, whose up-regulation is characteristic of reactive microglia (Ji et al., 2013), and for the expression of the *C4* gene coding for complement factor C4. Under the same conditions, reclFNB had no effect on the expression of the *ApoE* gene whose up-regulation is a main trait of disease associated microglia (DAM) (Butovsky & Weiner, 2018; Keren-Shaul et al., 2017). In the case of the genes associated with a pro-inflammatory response, the up-regulation induced by reclFNB was transient, diminishing after

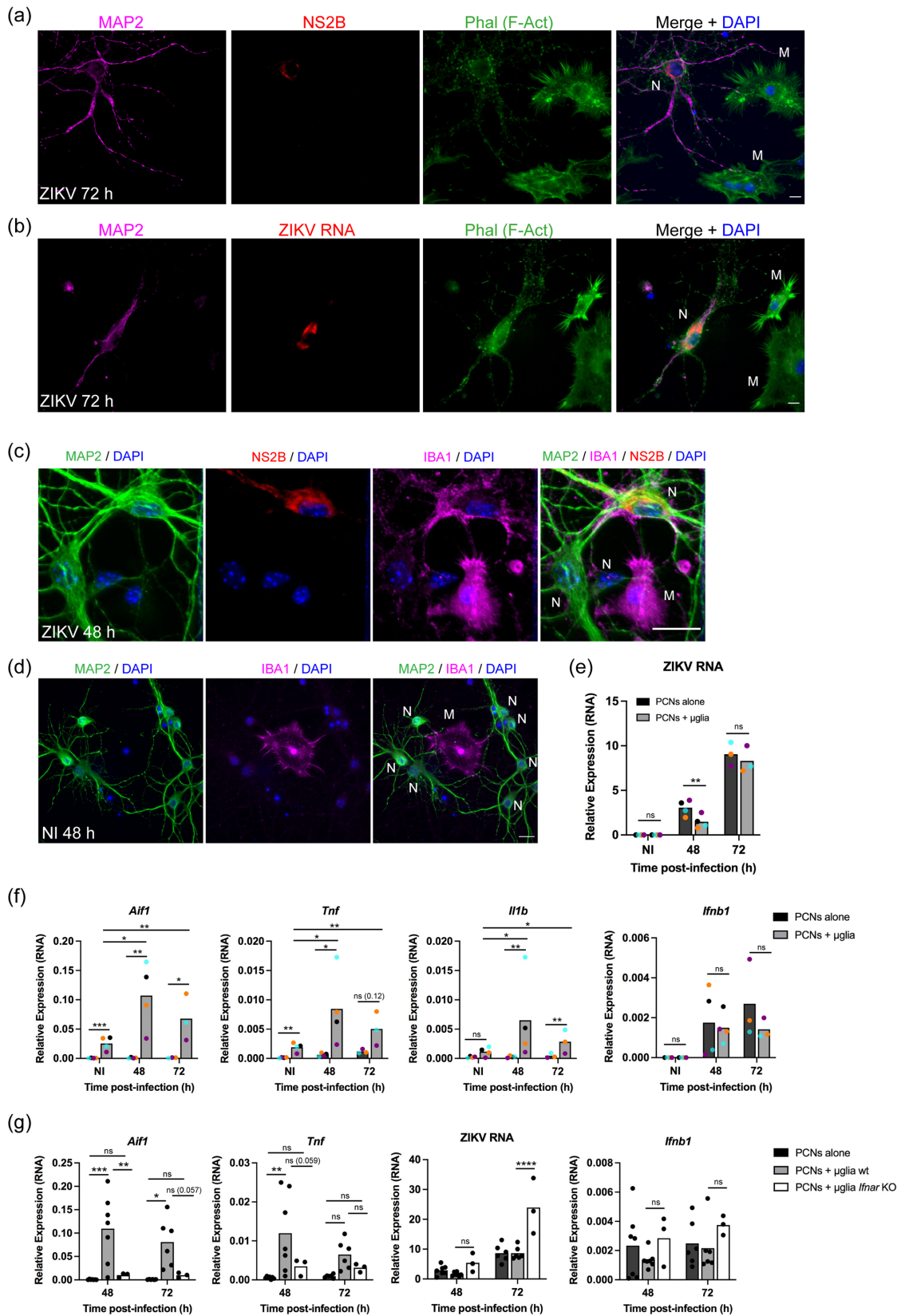


FIGURE 3 Legend on next page.

24 h of treatment, as it was also the case for some ISGs such *Isg15* and *Eif2ak2* (coding for kinase PKR) including the expression of the *Usp18* gene (Figure S2) that codes for the main long-lasting inhibitor of IFNAR signaling (Schneider et al., 2014).

Results shown here demonstrate that IFNs-I secreted by ZIKV-infected neurons as well as treatment with recIFNB directly induce a strong response in microglia significantly enhancing their phagocytic capacity as well as their capacity to mount a pro-inflammatory response. However, the transcriptional effect of recIFNB on microglial cells cultured alone was only transient.

3.2 | A prolonged neuron/microglia crosstalk leads to a sustained IFNs-I dependent microglia response in the context of ZIKV infection

In order to analyze the capacity of ZIKV-infected neurons to induce a sustained response in microglial cells, we performed primary co-cultures of neurons and microglia (with a neuron: microglia ratio of 5:1) that were either not exposed (NI) or exposed to ZIKV. After 48 and 72 h, the cells were fixed and analyzed by immunofluorescence (Figure 3a–d) while in parallel, the expression of ZIKV RNA and of genes associated with reactive microglia was assessed by RT-qPCR (Figure 3e–g).

In agreement with previous results obtained by our group and others (Figueiredo et al., 2019; Hayashida et al., 2019; Manet et al., 2022), neurons (labeled N), but not microglial (labeled M) cells were infected by ZIKV (Figure 3a,b). At 72 h p.i., ZIKV NS2B protein (Figure 3a) or RNA (Figure 3b) were detected within neurons but not in microglial cells (Figure 3a,b). Non-infected (NI) microglial cells were occasionally seen surrounding the soma and nucleus of a ZIKV-infected neuron (Figure 3c) similarly to what has been described in the case of neuronal corpse removal by microglia in vivo (Damisah et al., 2020). This was not observed in the absence of infection even when a microglial cell was seen positioned closely to neurons (Figure 3d).

Consistently with the absence of infection of microglial cells, the amount of ZIKV RNA detected by qPCR was not higher in co-cultures than in neurons cultured alone (Figure 3e). On the contrary, it was lower at 48 h p.i. in the presence of microglia suggesting that microglial cells could alleviate, at least transiently, the burden of ZIKV RNA present in ZIKV-infected neurons (Figure 3e).

In order to assess the capacity of ZIKV-infected neurons to induce a sustained microglial response, we measured the expression of the *Aif1*, *Tnf* and *Il1b* genes at 48 and 72 h p.i. (Figure 3f). As expected for genes expressed by microglia rather than neurons, their expression was observed under co-culture conditions and not in neurons cultured alone (Figure 3f). In agreement with the activation of a sustained microglial response induced by ZIKV-infected neurons, a significant up-regulation of the expression of these genes was observed in co-cultures at 48 h that persisted up to 72 h p.i. compared with their respective expression levels measured in the absence of ZIKV (NI) (Figure 3f). A sustained expression of the *Ifnb1* gene was observed until 72 h p.i. with no significant differences observed between neurons cultured alone or co-cultured with microglial cells (Figure 3f), suggesting that RNAs coded by *Ifnb1* were mainly produced by ZIKV-infected neurons.

In order to test the role of microglia IFNs-I signaling in their sustained response to ZIKV-infected neurons, neurons were co-cultured in parallel with microglial cells either wild type (wt) or defective for the IFNAR receptor (*Ifnar* KO) (Figure 3g). The activation of the expression of the *Aif1* and *Tnf* genes observed in co-cultures with wt microglia was absent with *Ifnar* KO microglia (Figure 3g), demonstrating the main role of microglial IFNAR signaling in their response to ZIKV-infected neurons. The decreased *Aif1* and *Tnf* gene expression in co-cultures with *Ifnar* KO compared to wt microglia was not related to a decrease of ZIKV RNA or *Ifnb1* gene expression (Figure 3g) that were either increased (ZIKV RNA at 72 h p.i.) or not significantly affected. Also under the same conditions, ZIKV had no effect on the expression of the *Cx3cr1* gene, a marker specific of microglial cells (Figure S3).

Together with confirming the effect of recIFNB (Figure 2) and of IFNs-I secreted by ZIKV-infected neurons (Manet et al., 2022, Figure 5) in activating a pro-inflammatory response in microglial cells, results obtained with co-cultures demonstrate that the IFN-I dependent response of microglial cells to ZIKV-infected neurons can be sustained under conditions of prolonged neuron/microglia crosstalk.

3.3 | PKR regulates the inflammatory response and phagocytic capacity of reactive microglia

In order to unravel the mechanism underlying the reactivity of microglial cells to IFNs-I, we questioned the potential role of kinase PKR

FIGURE 3 ZIKV infection of neurons co-cultured with microglia leads to the sustained activation of a pro-inflammatory response in non-infected microglia. Primary co-cultures of neurons (PCNs) and microglia (μ glia) (either wild type (wt) or *Ifnar*KO) were either non- (NI) or ZIKV-infected (ZIKV) at a multiplicity of infection (MOI) of 5. At indicated times p.i., cells were fixed and labeled for immunofluorescence analysis (a–d) and in parallel, RNAs were collected for gene expression analysis (e–g). (a, b) Neurons were labeled with anti-MAP2, ZIKV was labeled with either anti-NS2B or a fluorescent probe specific of the positive strand of ZIKV RNA, filamentous Actin (F-Act) was labeled with phalloidin and DNA with DAPI. (c, d) Neurons were labeled with anti-MAP2, ZIKV was labeled with anti-NS2B, microglia was labeled with anti-IBA1 and DNA with DAPI. N = neurons and M = wt microglia. Scale bars = 10 μ m. (e–g) RNAs from neurons (PCNs) cultured either alone or co-cultured with wt or *Ifnar*KO microglia (μ glia) were collected at 48 and 72 h p.i. RNA levels of the indicated genes were determined by RT-qPCR with respect to *Rplp0* used as reference gene. (e, f) Bars represent means with symbols corresponding to each independent experiment shown in different colors and significance assessed by ratio paired *t*-test. (g) Bars represent means with symbols corresponding to each independent experiment with significance assessed by two-way ANOVA Sidak's multiple comparison test. *p*-value <0.0001 (****), <0.001 (***), <0.01 (**), <0.05 (*), and ns = not significant.

that positively regulates the expression of pro-inflammatory genes (Gal-Ben-Ari et al., 2019) and that is encoded by a major ISG (Schneider et al., 2014) whose expression is up-regulated following treatment of PCMCs cells with CM_ZIKV (Manet et al., 2022, Figure 5) or recIFNB (Figure 2). To this aim, PCMCs were treated with either the C16 inhibitor of PKR (iPKR) or DMSO during 1 h before adding conditioned media from non- (CM-NI) or ZIKV-infected (CM_ZIKV) neurons. The capacity of PCMCs to express pro-inflammatory genes and phagocytose C3-SRBCs was assessed 6 h after adding conditioned media. A 6 h treatment of PCMCs with CM_ZIKV in the presence of DMSO induced a significant or near significant up-regulation of genes coding for pro-inflammatory and complement factors such as *Tnf*, *Nos2*, *Ccl2*, *C3*, and *C4* (Figure 4a) similarly to results obtained with CM_ZIKV in the absence of DMSO (Manet et al., 2022, Figure 5). The capacity of CM_ZIKV to induce the expression of these genes was significantly inhibited when microglial cells were previously incubated with iPKR.

Treatment with iPKR also completely inhibited the robust expression of the ISGs *Irf7* and *Isg15* induced by IFNs-I present in CM from ZIKV-infected neurons (Figure 4b; Manet et al., 2022, Figure 5). More surprisingly, iPKR also inhibited the low but significant expression of the *Ifnb1* gene induced following treatment with conditioned media from ZIKV-infected neurons (Figure 4b), demonstrating a major role for PKR in regulating not only microglia's pro-inflammatory response but also its IFNs-I gene expression and response that occurred in the absence of ZIKV replication (Figure 5d). Under the same conditions, iPKR had no effect on the expression of the *Clec7a* gene whose expression was not significantly affected after a 6 h treatment with CM_ZIKV + DMSO (Figure 4c) and also had no significant effect on the expression of the *Cd11b* gene, coding for one of the subunits of the C3 receptor, that was weakly but significantly induced following treatment with CM_ZIKV + DMSO (Figure 4c). These results are in agreement with those obtained in the context of PCMCs treated with recIFNB in the presence or absence of iPKR (Figure 5a).

In Figure 4d are shown the results of phagocytosis in the presence or absence of iPKR. We reproduce here in the presence of DMSO, the results previously obtained in the absence of DMSO (Figure 1) confirming the activator effect of the conditioned media from ZIKV-infected neurons (CM_ZIKV) on the C3-dependent phagocytic capacity of microglial cells. The treatment with iPKR significantly prevented the increase in the phagocytosis index induced by CM_ZIKV (Figure 4d).

Overall, the results obtained in vitro with PCMCs in the presence of iPKR identified PKR as the critical factor responsible of the up-regulation of the phagocytic capacity and the pro-inflammatory response of microglial cells induced by IFNs-I produced by ZIKV-infected PCNs.

3.4 | In vivo, PKR plays a major role in regulating the reactivity of non-infected microglia to IC ZIKV infection

The effect of the C16 inhibitor of PKR (iPKR) on the response of microglial cells to ZIKV infection was then tested in vivo on the Collaborative Cross mouse strain CC071 that we have previously

characterized as developing a strong microglia response 6 days post ZIKV infection (Bourdon et al., 2023; Manet et al., 2020; Manet et al., 2022). Immunofluorescence analysis of the brains of IC ZIKV-infected mice confirmed the strong response of microglia to ZIKV-infection in the CA region of the hippocampus at 6 days post-infection (dpi). Reactive microglial cells remained visible in this region of the brain at 9 and 15 dpi (Figure 5a) even though the presence of NS2B was no longer detected and ZIKV RNA replication stopped (Figure 5b). The persistency of this response observed by immunofluorescence at the cell level (Figure 5a) was confirmed at the transcriptional level by the persistent significant up-regulation of the expression of the microglial *Aif1* gene coding for IBA1 (Figure 5b).

In order to test the role of PKR on microglia's response to ZIKV infection in vivo, NI and ZIKV-IC infected CC071 mice were treated with C16 (iPKR) or DMSO by IP injection 45 min before and 3 days after IC infection. The animals were sacrificed at 6 dpi, one hemisphere was used for gene expression analyses and the other for immunofluorescence. RNAs were purified from total brain extracts and the expression of genes of interest was measured by RT-qPCR (Figure 6a-d). Treatment with iPKR significantly reduced the increased expression of genes associated with a pro-inflammatory response induced 6 days after IC ZIKV infection. This was the case of the genes: *Cxcl10*, *Nos2*, *Ccl2*, *Ccl5*, and *Il1b* with a significant or near significant inhibitory effect also observed for the *C4* and *C3* genes coding for the corresponding complement factors (Figure 6a). By contrast, we did not observe a significant effect of iPKR on the ZIKV-induced expression of the *Tnf* and *Il6* genes (Figure 5b). A significant iPKR-dependent inhibitory effect was observed for the ZIKV-induced expression of the *Aif1* gene (Figure 6b) whereas, under the same conditions, treatment with iPKR had no effect on the expression of genes not affected by ZIKV infection such as *Bdnf* and *Mef2c* (Figure 5b). In agreement with results obtained in vitro (Figure 4c), iPKR had no significant effect on the expression of the *Cd11b* gene induced following ZIKV infection (Figure 5b). The inhibitory effect of iPKR was not a consequence of either a diminution of ZIKV RNA (Figure 6c) or of the expression of the *Ifnb1* gene and of major ISGs (*Ilna4*, *Isg15*, *Eif2ak2*) that were not significantly affected by iPKR treatment (Figure 6d). Correlation analysis of the expression of genes related to a pro-inflammatory response (*Il1b* and *C4*) and microglia reactivity (*Aif1*) that were significantly affected after iPKR treatment, showed that their expression (as measured under NI + iPKR and ZIKV + DMSO conditions) was positively correlated with ZIKV RNA content (Figure 6e). However, the coefficient and significance of the correlation was stronger when the expression of these genes was plotted against the expression of the *Eif2ak2* gene, itself positively correlated to ZIKV RNA (Figure 6e). This is in agreement with a mechanism where ZIKV induces a pro-inflammatory response and the reactivity of microglia through PKR.

At the cellular level, under ZIKV + DMSO conditions, the microglial cells present within the region of infection displayed a condensed morphology with a large cellular body and thick, short, weakly ramified processes (Figure 6f), which is often associated with "hyper-reactive" microglial cells (Savage et al., 2019; Schwabenland et al., 2021). Interestingly, treatment with iPKR seemed to modify the morphology of microglial cells present within the region of infection that adopted

under ZIKV + iPKR conditions a morphology resembling that most commonly described for homeostatic microglia (Savage et al., 2019; Schwabenland et al., 2021) with a small cellular body and multiple, thin ramified processes (Figure 6f).

The effect of ZIKV infection and iPKR on microglia's morphology was further assessed by anti-Iba1 immunohistochemistry on brain sections of the same mice analyzed in Figure 6. Whole slide images of the brains were analyzed using the QuPath software in order to measure the cell body area of microglial cells present either in the whole

hippocampal region (Figure 7a, yellow selection) or more specifically in the CA region (Figure 7a, green selection) that corresponds to the region of the hippocampus where we have observed the highest density of NS2B+ neurons 6 days post IC ZIKV infection (Figures 5 and 6f). The quantified cell body area of microglial cells in the whole hippocampus (Figure 7b, yellow selection) was not significantly increased after ZIKV infection (Figure 7c). However, when the cell body area of microglial cells was analyzed more specifically in the CA region of the hippocampus, a significant increase of microglia's cell body area was

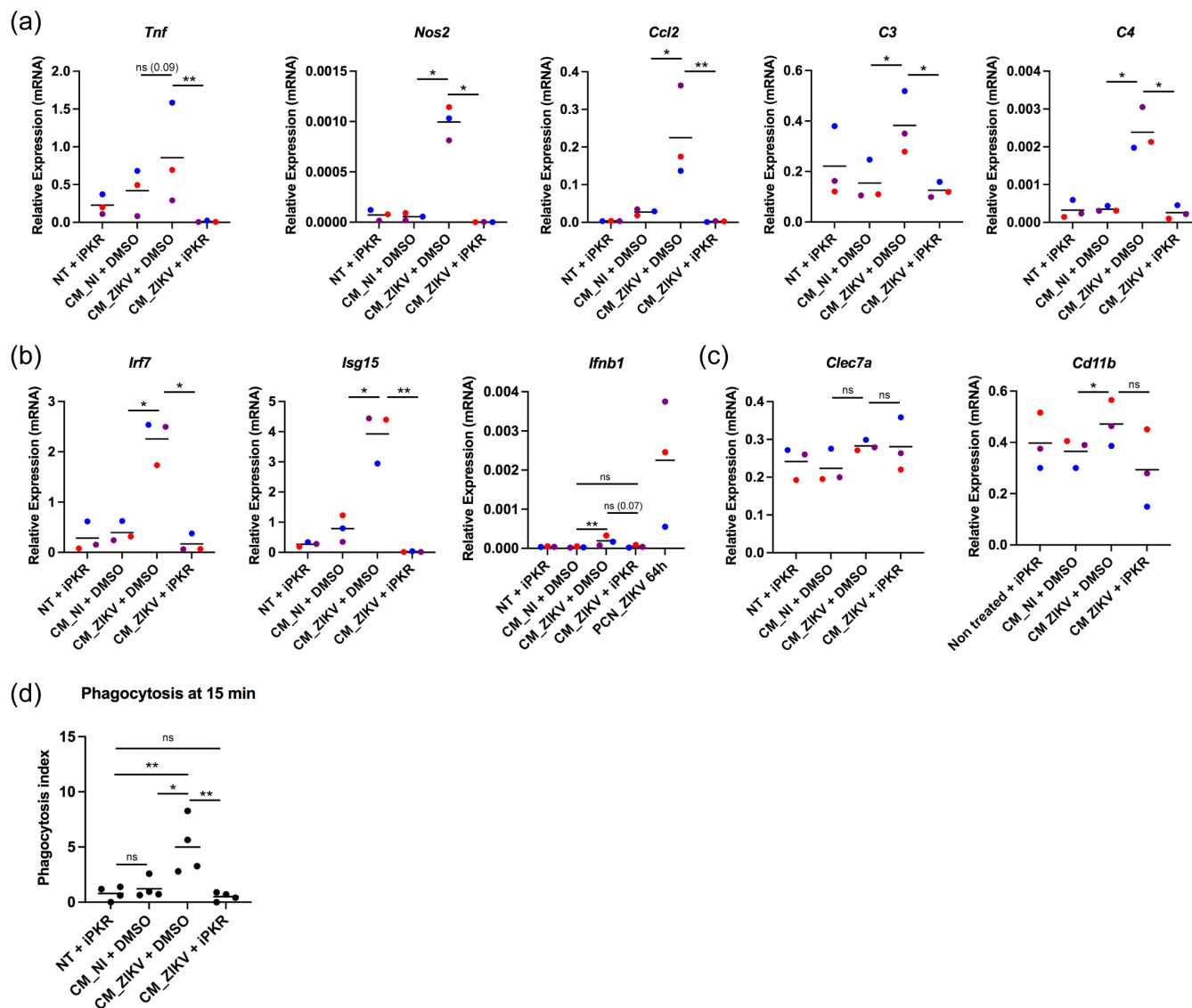


FIGURE 4 Kinase PKR is a major regulator of non-infected microglia's inflammatory and phagocytic response to ZIKV-infected neurons. Primary cultured microglial cells (PCMCs) were incubated with DMSO or the inhibitor of PKR (C16) for 1 h before being either non-treated (NT), treated with conditioned media from non- (CM_NI) or ZIKV-infected (CM_ZIKV) primary cultured neurons or ZIKV alone (NT_ZIKV) for 6 h. In Figure 4a–c are shown the qPCR results obtained from three independent primary cultures of microglia treated with conditioned media collected from three independent primary cultures of neurons. RNAs were collected and gene expression analysis was carried out by RT-qPCR with respect to *Rplp0* used as reference gene for genes associated with (a) the pro-inflammatory response, (b) IFN-I response with the level of *Ifnb1* expression present in the three ZIKV-infected PCNs from which the CMs were collected (PCN_ZIKV 64 h) also shown, (c) DAM response. Dot plots show means with one dot for each independent experiment represented in different colors. Significance was assessed by ratio-paired *t*-test. (d) After 15 min incubation with C3_SRBCs, phagocytosis index was determined as in Figure 1. Dot plots show means with one dot for each independent experiment. Significance was assessed by two-way ANOVA Tukey's multiple comparison test. *p*-value <0.01 (**), <0.05 (*), and ns = not significant; *p*-values near significance are indicated.

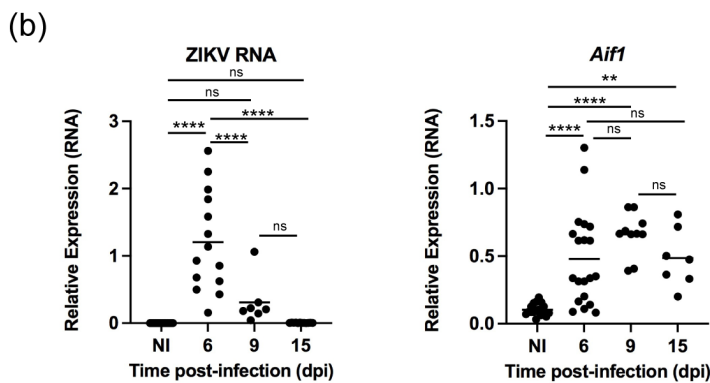
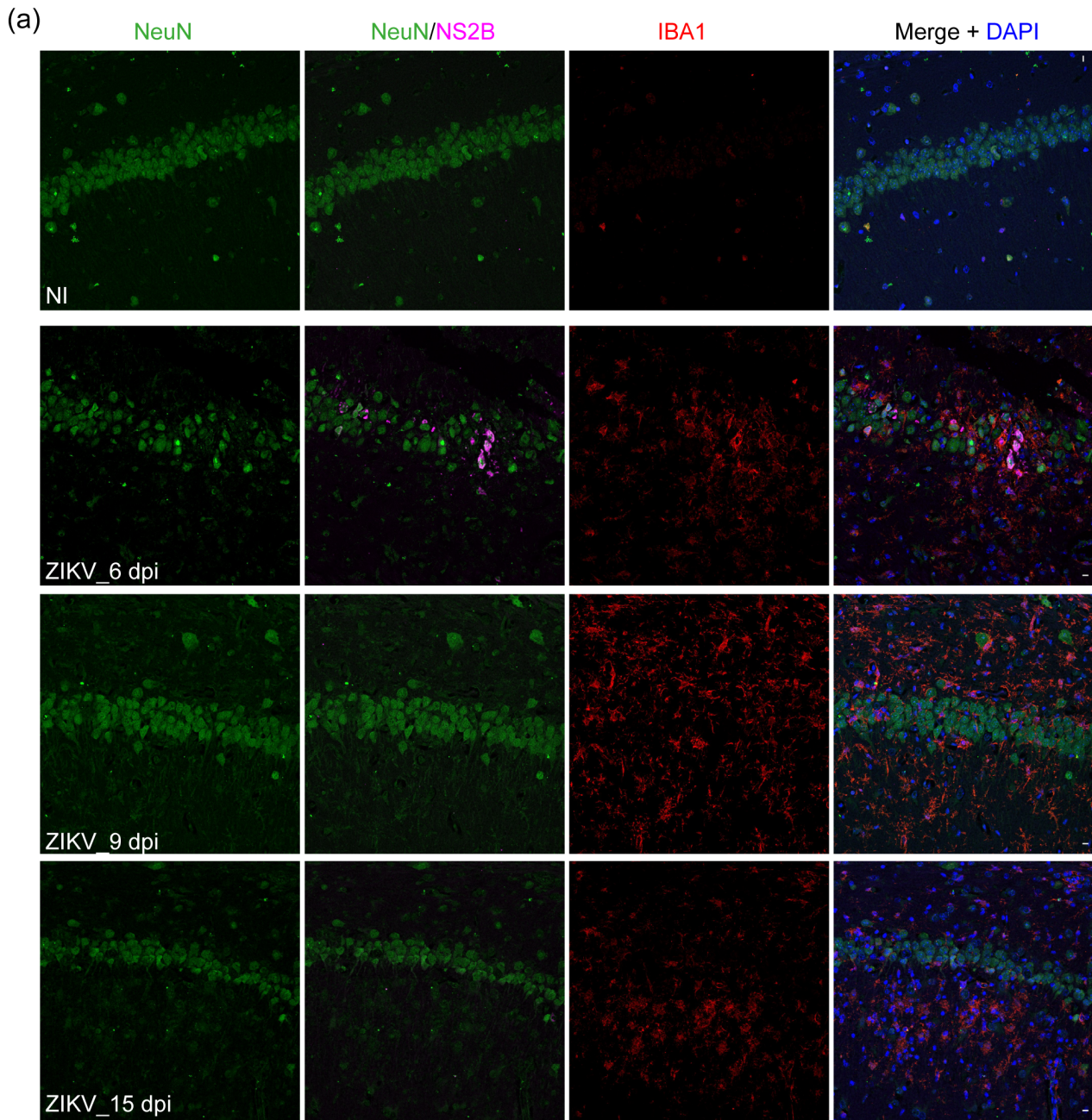


FIGURE 5 Legend on next page.

observed after ZIKV infection (Figure 7c) indicative of ZIKV predominantly affecting the morphology of microglial cells positioned near the region of infection. The significant enlargement of the cell body area induced by ZIKV infection in the CA1 region was lost after treatment with iPKR (Figure 7c). In agreement with a main role for PKR regulating microglial morphology, the average cell body area of microglial cells present in each CA region was significantly positively correlated with the expression of the *Eif2ak2* gene measured in the corresponding brain (Figure 7d). The correlation was weaker when the average cell body area was plotted against the ZIKV RNA content of the corresponding brain (Figure 7d) despite a strong positive correlation between *Eif2ak2* expression and ZIKV RNA content, indicative of ZIKV infection affecting microglial morphology not directly but through PKR. Following ZIKV infection, some microglial cells (red arrow in Figure 7b, ZIKV-DMSO), were seen closely surrounding neuronal nuclei similarly to what we have observed in ZIKV-infected primary co-cultures of neurons and microglia (Figure 3c). Alongside with the quantification of the cell body area, we also quantified the number of microglial cells in the regions of interest. Even though a trend towards an increase of the number of microglial cells was observed after ZIKV infection, the differences observed between the different conditions analyzed remained non-significant either in the whole hippocampus or the CA region (Figure 7e). Similar densities of microglial cells were observed in the whole hippocampus and the CA region (Figure 7e) showing that, while ZIKV infection enhanced the expression of *Aif1* and pro-inflammatory genes and modified the morphology of microglial cells in the region of infection, through a PKR-dependent mechanism, it did not significantly affect the number of microglial cells present within this region.

Overall, in vivo, PKR appeared as a major regulator of the main transcriptional and morphological traits adopted by reactive NI microglia in response to IC ZIKV infection such as the up-regulation of the expression of genes coding for IBA1, for pro-inflammatory and complement factors and the adoption of an ameboid-like morphology.

3.5 | Endogenous IFNs-I regulate the inflammatory response and phagocytic capacity of virus-infected microglia through PKR

In comparison to the effect of exogenous IFNs-I (either reIFNB or IFNs-I produced by ZIKV-infected neurons) on microglial cells, we

questioned the capacity of endogenous IFNs-I produced by virus-infected PCMCs to activate the pro-inflammatory response and phagocytic capacity of microglia. For this, PCMCs treated or not with the anti-IFNAR antibody were infected with the Newcastle Disease Virus (NDV), an avian paramyxovirus that induces a strong IFNs-I response in murine cells. Five hours after infection, gene expression (Figure 8a-c) and phagocytosis of C3-SRBCs (Figure 8d) were analyzed. Infection of PCMCs with NDV induced a strong IFNs-I response that, as expected, was inhibited by anti-IFNAR antibodies (Figure 8a). NDV infection also induced the expression of the genes *Il6*, *Nos2*, *Cxcl10*, *Ccl2*, *Tnf*, and *C3* that was significantly neutralized by the anti-IFNAR antibody (Figure 8b) with a near significant effect observed for the *Tnf* gene (Figure 8b). Under the same conditions, treatment with anti-IFNAR had no effect on the expression of the *C1qa* and *Cd11b* genes that were not significantly affected following NDV infection or anti-IFNAR treatment (Figure 8c) in agreement with results showing the lack of effect of reIFNB treatment on *Cd11b* expression in microglial cells (Figure S7b). PCMCs's phagocytosis index that was significantly increased 5 h after NDV infection (Figure 8d) was significantly reduced in the presence of anti-IFNAR antibody (Figure 8d). Thus, as previously shown following treatment of NI PCMCs with exogenous IFNs-I, we demonstrate here that endogenous IFNs-I produced by virus-infected PCMCs also regulate the expression of pro-inflammatory genes as well as the enhancement of the C3-dependent phagocytic capacity of microglial cells.

In order to test the role of PKR on the response of microglia to endogenous IFNs-I, PCMCs were incubated with iPKR 1 h before NDV infection. Results obtained following gene expression analysis (Figure 8e), demonstrated a main role for PKR in regulating NDV-induced expression of pro-inflammatory genes *C3*, *Il6*, and *Nos2*, while under the same conditions iPKR treatment had no significant effect on the expression of the *Cd11b* gene that was not affected by either NDV infection (Figure 8e) or anti-IFNAR treatment (Figure 8c). Treatment of PCMCs with iPKR also induced a significant decrease of the level of expression of the *Irfb1* and abolished the capacity of NDV infection to induce ISG (*Irf7*) expression (Figure 8f), while it did not affect NDV replication (Figure S6a).

We demonstrate here that, as in the case of exogenous IFNs-I, PKR plays a main role in regulating the ISGs expression, pro-inflammatory, and phagocytosis response induced by endogenous IFNs-I in NDV-infected microglia.

FIGURE 5 ZIKV infection induces a sustained microglia response in immunocompetent mice, in the absence of microglia infection. CC071 mice (5–6 weeks-old) were necropsied at days 6, 9, and 15 following IC inoculation of either NaCl or 10^5 FFU of ZIKV. One hemisphere was used for immunofluorescence and the other hemisphere was used for RNA extraction and gene expression analysis. (a) Brain sections of non-infected (NI) and ZIKV-infected (ZIKV) mice were labeled at 6, 9, and 15 days post-infection (dpi) with anti-NeuN (specific of neurons), anti-IBA1 (specific of microglia) and anti-NS2B (specific of ZIKV) antibodies and with DNA labeled with DAPI. Maximum intensity projection of confocal sections (z projection) and the corresponding merge images are shown. Scale bars = 10 μ m. (b) Levels of RNAs of ZIKV and the *Aif1* gene (coding for microglia's marker IBA1) were determined following RT-qPCR analysis of total brain extracts with respect to *Hrpt1* used as reference gene. Symbols represent individual mice. Dot plots show means with one dot for each brain and significance assessed by one-way ANOVA Tukey's multiple comparison test. p -value <0.0001 (****), <0.01 (**), and ns = not significant.

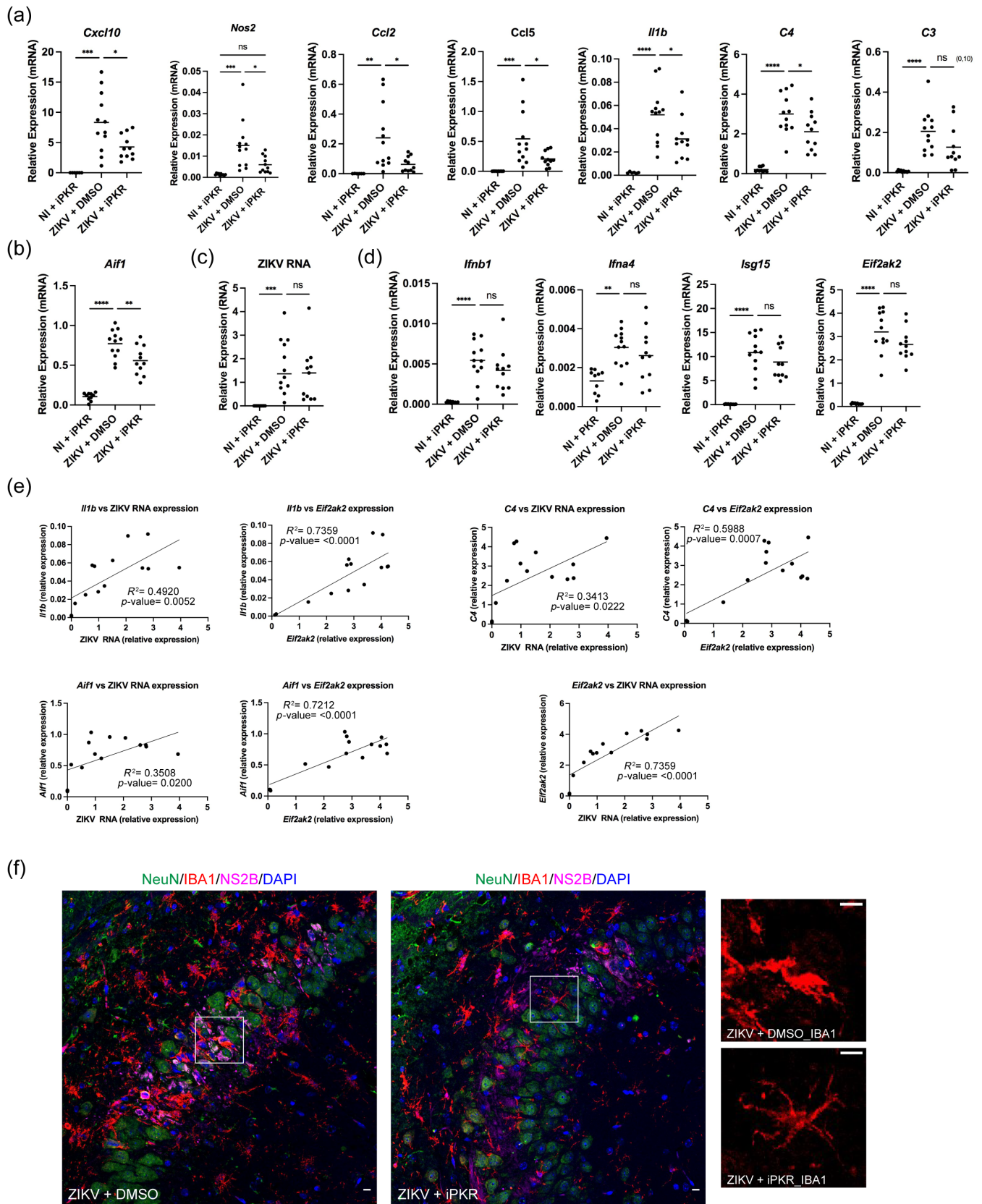


FIGURE 6 Legend on next page.

3.6 | PKR inhibition does not prevent ISG and pro-inflammatory gene expression in NDV-infected neurons

The role of PKR in regulating ISG and pro-inflammatory gene expression previously demonstrated in microglial cells was also analyzed in neurons. For this, primary cultured neurons (PCNs) were infected with NDV in the presence or absence of iPKR under the same conditions used in the case of microglial cells. As previously shown (Manet et al., 2022, Figure S1), NDV infection induced an IFNB response in neurons as indicated by the up-regulation of the expression of the *Irfb1* and *Irf7* genes (Figure 8g). Contrary to results observed in microglial cells (Figure 8f), treatment with iPKR had no significant effect on the level of expression of *Irfb1* and did not prevent the significant up-regulation of *Irf7* induced by NDV in neurons (Figure 8g). Similarly, iPKR treatment did not prevent the significant up-regulation of *Ccl2* and *C3* genes induced by NDV in neurons (Figure 8g), contrary to what was observed in microglial cells for the *C3* gene (Figure 8e). As in the case of microglial cells, iPKR had no effect on NDV replication in neurons (Figure S6a). Of note, neurons displayed a much lower basal level of *Eif2ak2* gene expression compared with microglia (Figure S6b).

Thus, the strong dependency of reactive microglia on PKR for the induction of the expression of the genes of the IFNB and pro-inflammatory response was shown here to be specific of microglial cells compared to neurons.

3.7 | PKR is a major regulator of STAT1 phosphorylation in microglial cells

In order to question the mechanism through which PKR could vehicle the response of microglia to IFNs-I, we analyzed the capacity of PKR to regulate the phosphorylation of the signal transducer activator of transcription STAT1 that regulates IFNAR signaling (Schneider et al., 2014) and has been associated with a pro-inflammatory state of microglia (Butturini et al., 2019; Rangaraju et al., 2018). In addition, we analyzed the phosphorylation of the inhibitor of NF- κ B (I κ B) whose phosphorylation by PKR is a well described mechanism that links PKR to the induction of the expression of pro-inflammatory

genes (Gal-Ben-Ari et al., 2019). PCMCs treated with either DMSO or iPKR were infected with NDV (Figure 9a,b,e,f) or treated with conditioned media collected from non-infected (CM_NI) or ZIKV-infected (CM_ZIKV) PCNs (Figure 9c,d,g,h). Proteins extracts collected 5 h after NDV infection and 6 h after incubation with conditioned media were analyzed by Western blot. Infection with NDV and incubation with CM_ZIKV significantly induced the phosphorylation of STAT1 (Stat1ph) (Figure 9a-d) whereas, no significant phosphorylation of I κ B (I κ Bph) was observed under the same conditions (Figure 9e-h).

Treatment with iPKR significantly inhibited the phosphorylation of STAT1 induced by NDV infection (Figure 9a,b) and CM_ZIKV (Figure 9c,d). The effect was dose dependent with the phosphorylated form of STAT1 (Stat1ph) no longer detected in protein extracts from NDV-infected PCMCs treated with 50 μ M of iPKR, that corresponds to the concentration of iPKR used in Figures 4 and 7. Under the same conditions, iPKR treatment had no effect on the phosphorylation of the transcription factor IRF3 (IRF3ph), a main regulator of *Irfb1* gene expression, induced following NDV-infection (Figure 9a). Interestingly, no phosphorylation of STAT1 was detected in NDV-infected PCNs that expressed very low levels of total STAT1 compared to microglial cells (Figure 9i).

3.8 | PKR regulates IRF1 protein level in primary cultured microglial cells and *Irf1* gene expression in brain extracts of ZIKV-infected mice

Homodimers of phosphorylated STAT1 regulate the expression of transcription factor IRF1 (Forero et al., 2019; Feng et al., 2021) that is a major regulator of the phagocytosis, inflammation, and DAM transcriptional profiles of microglia (Gao et al., 2019). Particularly, IRF1 is necessary to establish the reactive state of microglia in response to stimulation by lipopolysaccharide (LPS) regulating LPS-stimulated phagocytosis, LPS-induced expression of genes such as *Nos2*, *IL6*, *Ccl2*, *Ccl5* as well as the amoeboid-like morphology adopted by microglia in response to LPS (Yang et al., 2022). In order to question the potential role of IRF1 in microglia reactivity to NDV and CM_ZIKV, the level of IRF1 was measured by WB in protein extracts from PCMCs and neurons non- and NDV-infected as well as from PCMCs incubated with different neuronal conditioned media. Western blot

FIGURE 6 In vivo, kinase PKR regulates the pro-inflammatory and *Aif1* gene expression response to ZIKV infection. CC071 mice (5–6 weeks-old) were treated with DMSO or the inhibitor of PKR (iPKR) 1 h before and 3 days after IC inoculation of either NaCl (NI) or 10^5 FFU of ZIKV. Mice were necropsied 6 days after infection with one hemisphere used for immunofluorescence and the other one used for RNA extraction and gene expression analysis. (a–d) Levels of RNAs purified from whole brain extracts were determined by RT-qPCR with respect to *Hprt1* used as reference gene. Symbols represent individual mice with $n = 10$ (NI + iPKR), $n = 12$ (ZIKV + DMSO) and $n = 11$ (ZIKV + iPKR). Dot plots show means with one dot for each brain and significance assessed by one-way ANOVA Tukey's multiple comparison test. p -value <0.0001 (****), <0.001 (***), <0.01 (**), <0.05 (*) and ns = not significant; p -values near significance are indicated. (e) Correlation analysis of the expression levels of the *Il1b*, *C4*, and *Aif1* genes (as determined in NI + iPKR and ZIKV + DMSO conditions) with either *Eif2ak2* expression or ZIKV RNA expression. Symbols represent individual mice. (f) Brain sections of ZIKV-infected mice treated either with DMSO (ZIKV + DMSO) or PKR inhibitor C16 (ZIKV + iPKR) were labeled with anti-NeuN (specific of neurons), anti-IBA1 (specific of microglia) and anti-NS2B (specific of ZIKV) antibodies and with DNA labeled with DAPI. Merge images of maximum intensity projection of confocal sections (z projection) are shown. Scale bars = 10 μ m.

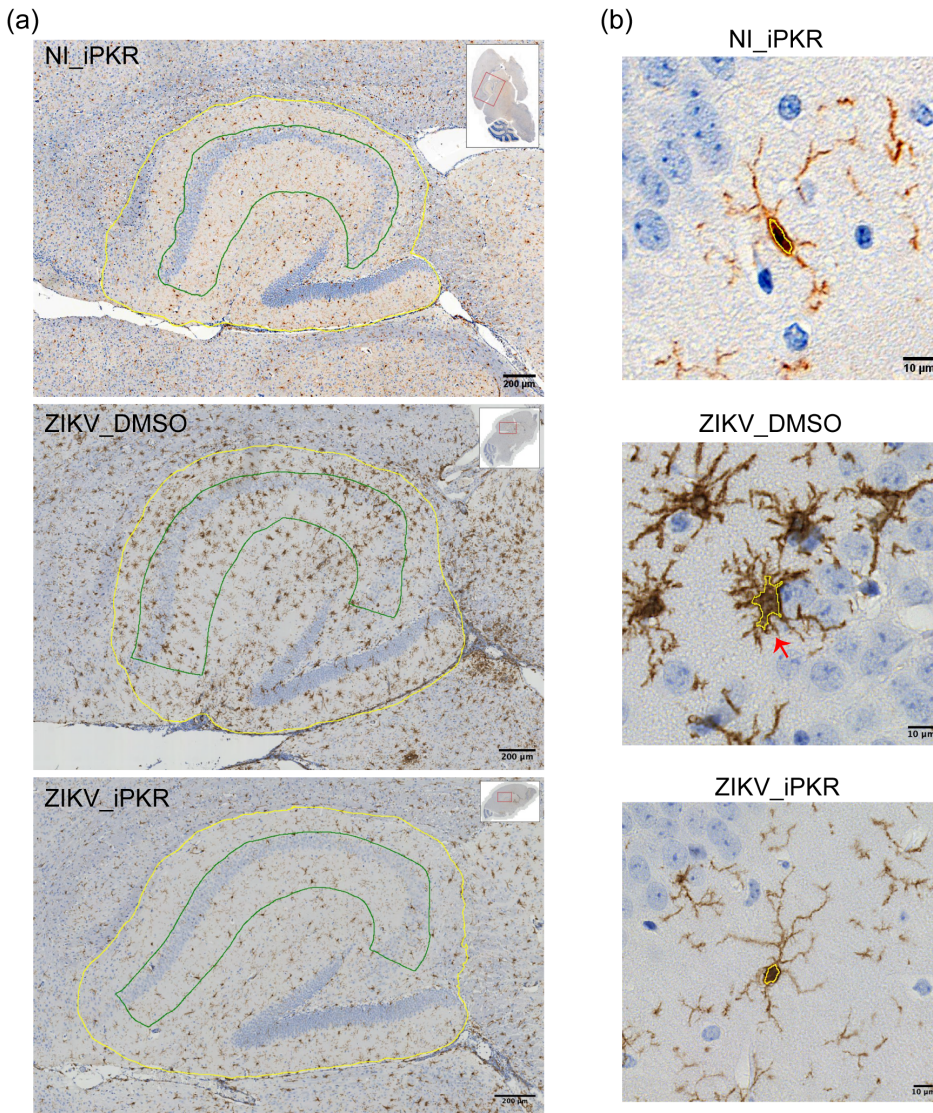
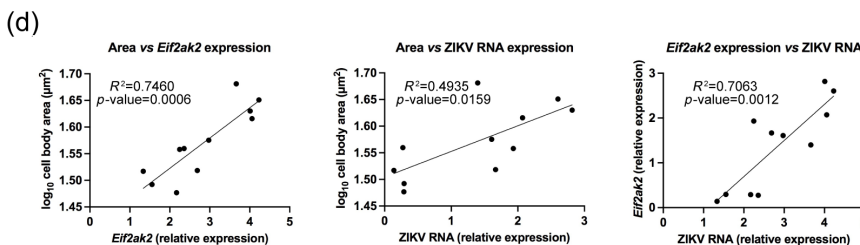
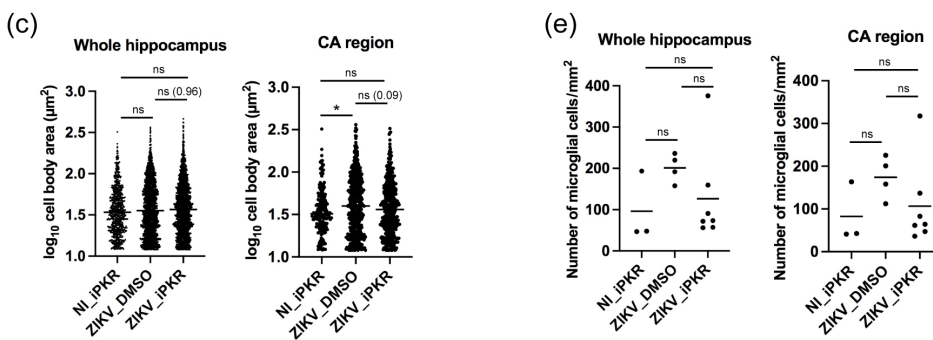


FIGURE 7 PKR regulates the morphological transformation of microglia induced by ZIKV infection. Immunohistochemical analysis of 3 NI_iPKR, 4 ZIKV_DMSO and 7 ZIKV_iPKR mice among those analyzed in Figure 6.

(a) Representative images of brain sections stained with an anti-IBA1 immunoperoxidase antibody. Images obtained with a slide scanner microscope were analyzed using the QuPath software in order to assess the cell body area and the number of microglial cells in the region of the whole hippocampus (yellow selection) and the CA (green selection).

(b) Enlarged representative images of microglial cells with the cell body region selected by QuPath indicated in yellow. (c) Cell body areas of independent microglial cells as determined using QuPath. Symbols represent individual microglial cells. In the case of the whole hippocampus, $n = 735$ (NI_iPKR), $n = 1763$ (ZIKV_DMSO) and $n = 1988$ (ZIKV_iPKR) cells. In the case of the CA region, $n = 188$ (NI_iPKR), $n = 477$ (ZIKV_DMSO) and $n = 437$ (ZIKV_iPKR) cells. The values were converted to \log_{10} . Dot plots show medians with significance assessed by the non-parametric Mann-Whitney test with p -value < 0.05 (*) and ns = not significant; p -values for ZIKV-DMSO versus ZIKV_iPKR conditions are indicated.



(d) Correlation analysis of the average cell body area of microglial cells present in each CA region with either *Eif2ak2* mRNA or ZIKV RNA expression measured in the corresponding brains. Symbols represent average values per brain. (e) Symbols represent individual mice with $n = 3$ (NI_iPKR), $n = 4$ (ZIKV-DMSO), and $n = 7$ (ZIKV_iPKR). Dot plots show means with significance assessed by one-way ANOVA Tukey's multiple comparison test with ns = not significant.

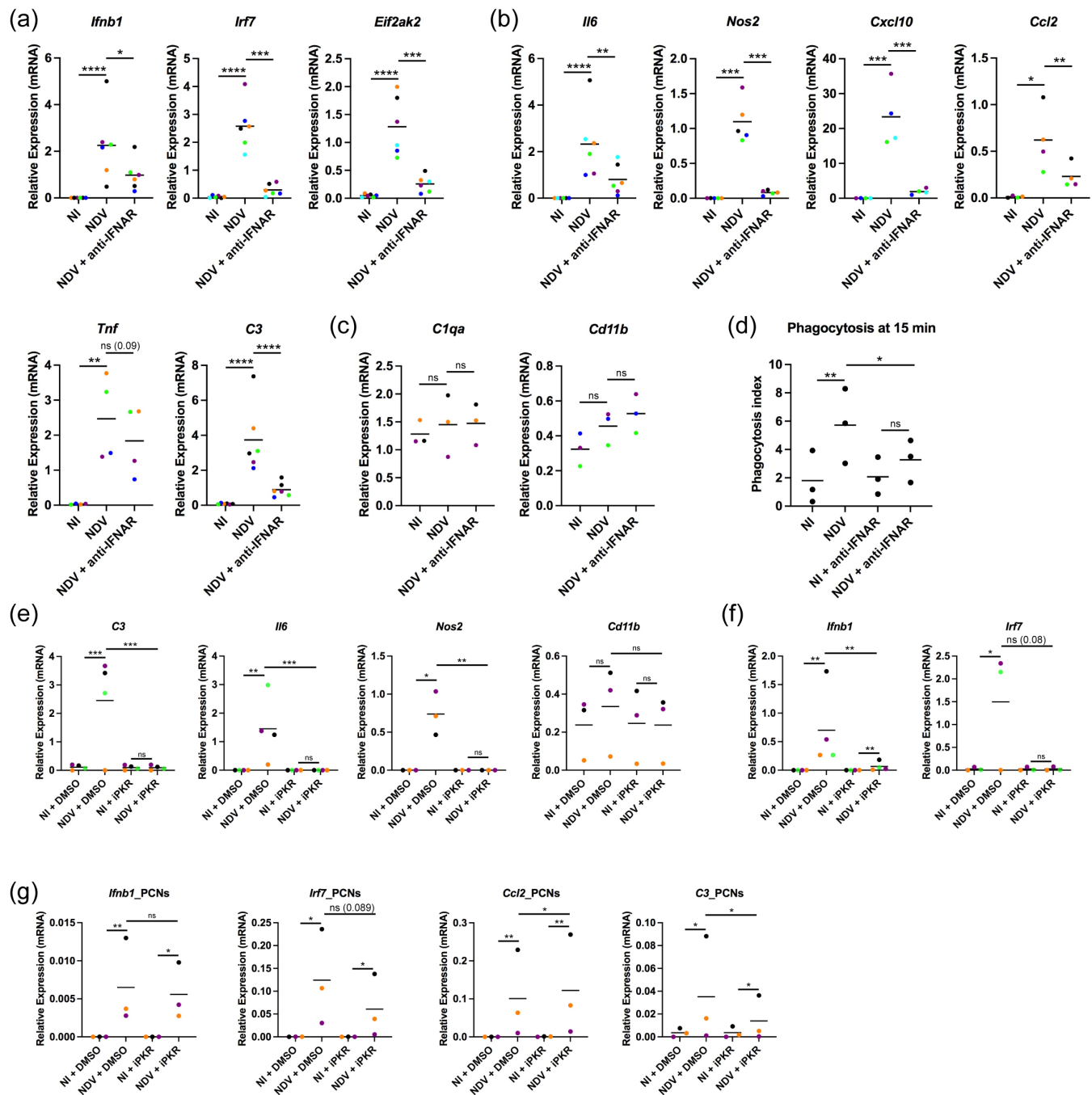


FIGURE 8 Endogenous IFNs-I increase the pro-inflammatory and phagocytic capacity of newcastle disease virus (NDV)-infected microglia. (a–d) Primary cultures of microglia (PCMCs) were either non-infected (NI) or infected with NDV in the presence or absence of anti-IFNAR antibody. (a–c) Gene expression analysis using RNAs collected 5 h post-infection were carried out by RT-qPCR using *Rplp0* as reference gene. Dot plots show means with one dot for each independent culture represented in different colors. Significance was assessed by ratio paired t test. p -value <0.0001 (****), <0.001 (***), <0.01 (**), <0.05 (*), and ns = not significant; p -values near significance are indicated. (d) After 15 min incubation with C3_SRBs, phagocytosis index was determined as in Figure 1. Dot plots show means with one dot for each independent experiment. Significance was assessed by two-way ANOVA Tukey's multiple comparison test. p -value <0.01 (**), <0.05 (*), and ns = not significant; p -values near significance are indicated. (e–g) PCMCs (e, f) or PCNs (g) were incubated with DMSO or the inhibitor of PKR (IPKR) 1 h before NDV infection. Gene expression analysis using RNAs from PCMCs and PCNs, collected 5 and 8 h post-infection respectively, were carried out by RT-qPCR using *Rplp0* as reference gene. Dot plots show means with one dot for each independent culture represented in different colors. Significance was assessed by ratio paired t test. p -value <0.001 (****), <0.01 (**), <0.05 (*) and ns = not significant; p -values near significance are indicated.

analysis of the protein level of IRF1 in non- and NDV-infected neurons and microglia revealed that microglial cells expressed high basal and NDV-induced levels of IRF1 protein whereas IRF1 was weakly detected in neurons (Figure 9j). An enhancement of the protein level of IRF1 was also observed in the presence of DMSO after stimulation of microglial cells with conditioned media from ZIKV-infected neurons compared with stimulation with conditioned media from NI neurons (Figure 9j). Treatment of microglial cells with iPKR under the conditions used for the inhibition of STAT1 phosphorylation induced by CM_ZIKV + iPKR in PCMCs (Figure 9c,d), completely inhibited the basal as well as the induced level of microglial IRF1 protein expression (Figure 9j).

While binding of IFNs-I to their IFNAR receptor leads to the phosphorylation of STAT1 and STAT2 and the formation of phosphorylated STAT1/STAT2 heterodimers (Schneider et al., 2014), the formation of phosphorylated STAT1/STAT1 homodimers and the subsequent induction of *Irf1* expression can occur in response to IFNs-I provided that sufficient levels of phosphorylated STAT1 are induced (Forero et al., 2019). As shown in Figure 9k, treatment with recIFNB induced a robust expression of *Irf1* expression in PCMCs that was only weakly observed in PCNs (Figure 9k), which is in agreement with results shown in Figure 9i indicating higher amounts of total and phosphorylated STAT1 in PCMCs compared to PCNs.

The link between PKR and IRF1 was also tested *in vivo*. For this, the expression level of the *Irf1* gene was analyzed in brain extracts from ZIKV-infected adult immunocompetent mice treated with DMSO or iPKR described in Figure 6. As shown in Figure 9l, treatment with iPKR inhibited the expression of the *Irf1* gene (p -value = 0.08) induced in whole brain extracts following ZIKV infection while it had no effect (p -value = 0.54) on the ZIKV-induced expression of *Irf7* that does not depend on phosphorylated STAT1 homodimers or IRF1 for its expression (Forero et al., 2019). These results are indicative of a role for PKR in regulating ZIKV-induced *Irf1* expression in the brain of adult immunocompetent mice infected by ZIKV.

4 | DISCUSSION

Reactive microglial cells are characterized by their capacity to mount a pro-inflammatory response and to display an enhanced complement C3-dependent phagocytic capacity. The results presented in this study demonstrate the major role played by exogenous and endogenous IFNs-I in directly activating these two through microglia's IFNAR signaling and kinase PKR. A role for IFNAR-signaling in regulating microglia's reactivity has been previously described in the context of lymphocytic choriomeningitis virus (LCMV) infection (Nayak et al., 2013), murine prion disease (Nazmi et al., 2019) and in a murine model of AD (Roy et al., 2020; Roy et al., 2022). However, in these studies the direct effects of IFNs-I on microglia were not explored. Also in these studies, microglial cells were proposed to be at the origin of the expression of IFNs-I that in turn would signal other cell types of the brain, such as astrocytes for C3 expression (Roy et al., 2020) and neurons for neurotoxic pathology (Roy et al., 2022). By contrast,

we describe therein a mechanism where microglial cells are not the producers of IFNs-I but respond to IFNs-I produced by neurons. We demonstrate here that IFNs-I secreted by ZIKV-infected neurons directly activate the phagocytic capacity, pro-inflammatory state and IFN-I response of NI microglia through PKR. We also demonstrate a role for PKR in regulating the morphology of microglia *in vivo* mediating microglia's cell body enlargement upon ZIKV infection. By doing so, we unravel the mechanism controlling the ZIKV-induced activation of microglia in the brain of adult immunocompetent mice under conditions where neurons, but not microglial cells, are infected by the virus.

The binding of IFNs-I to their IFNAR receptor triggers the activation of kinases JAK1 and TYK2 that phosphorylate transcription factors STAT1 and STAT2 (Figure 10) predominantly leading to the formation of phosphorylated pSTAT1/pSTAT2 heterodimers (Schneider et al., 2014), which, in association with IRF9, regulate the expression of ISGs (among which the gene coding for PKR) and the innate antiviral response. By contrast, the expression of pro-inflammatory genes mainly relies on NF- κ B whose activation is not directly linked to IFNAR signaling and/or on the formation of phosphorylated pSTAT1/pSTAT1 homodimers that promote the expression of transcription factor IRF1 (Feng et al., 2021). These homodimers are mainly formed in response to IFN gamma (IFNG) (Schneider et al., 2014). However, even though underrepresented compared with heterodimers, pSTAT1/pSTAT1 homodimers can also be formed in response to type I IFNs provided that a sufficient amount of STAT1 is phosphorylated, leading to an IFN-I dependent induction of the expression of transcription factor IRF1 (Forero et al., 2019). Results obtained here with iPKR identified PKR as the major direct regulator of STAT1 phosphorylation in microglial cells either treated with CM_ZIKV or infected with NDV whereas under the same conditions, no significant effect was observed on I κ B phosphorylation necessary for the activation of NF- κ B.

The basal level of expression of the *Eif2ak2* gene is higher in microglial cells as compared to neurons (Figure 56b). This coincides with a low basal level of pSTAT1 detected in NI and NT PCMCs but not in neurons (Figure 9i), that could explain the basal level of IRF1 present in PCMCs even in the absence of induction (Figure 9j). We show here that within a short period of time (6 h post-treatment), iPKR down-regulates pro-inflammatory and ISGs expression levels induced by exogenous IFNs-I present in conditioned media from ZIKV-infected neurons (Figure 4). STAT1 and IRF1 have been described as main regulators of microglia's pro-inflammatory response and phagocytosis (Butturini et al., 2019; Gao et al., 2019; Rangaraju et al., 2018; Yang et al., 2022). Also an ISG such as *Lgals3bp* has been recently shown to regulate microglia's reactivity (Arutyunov et al., 2024). Thus, iPKR could rapidly negatively regulate the pro-inflammatory response and phagocytic capacity of microglia by affecting the basal and induced levels of p-STAT1 and IRF1 alongside with the induction of ISG expression. However, we cannot exclude that PKR could also contribute to phagocytosis through protein-protein interactions and/or protein phosphorylation.

The effect of PKR on IFN-I dependent microglia's activation could be maintained throughout a longer period of time through a two-step

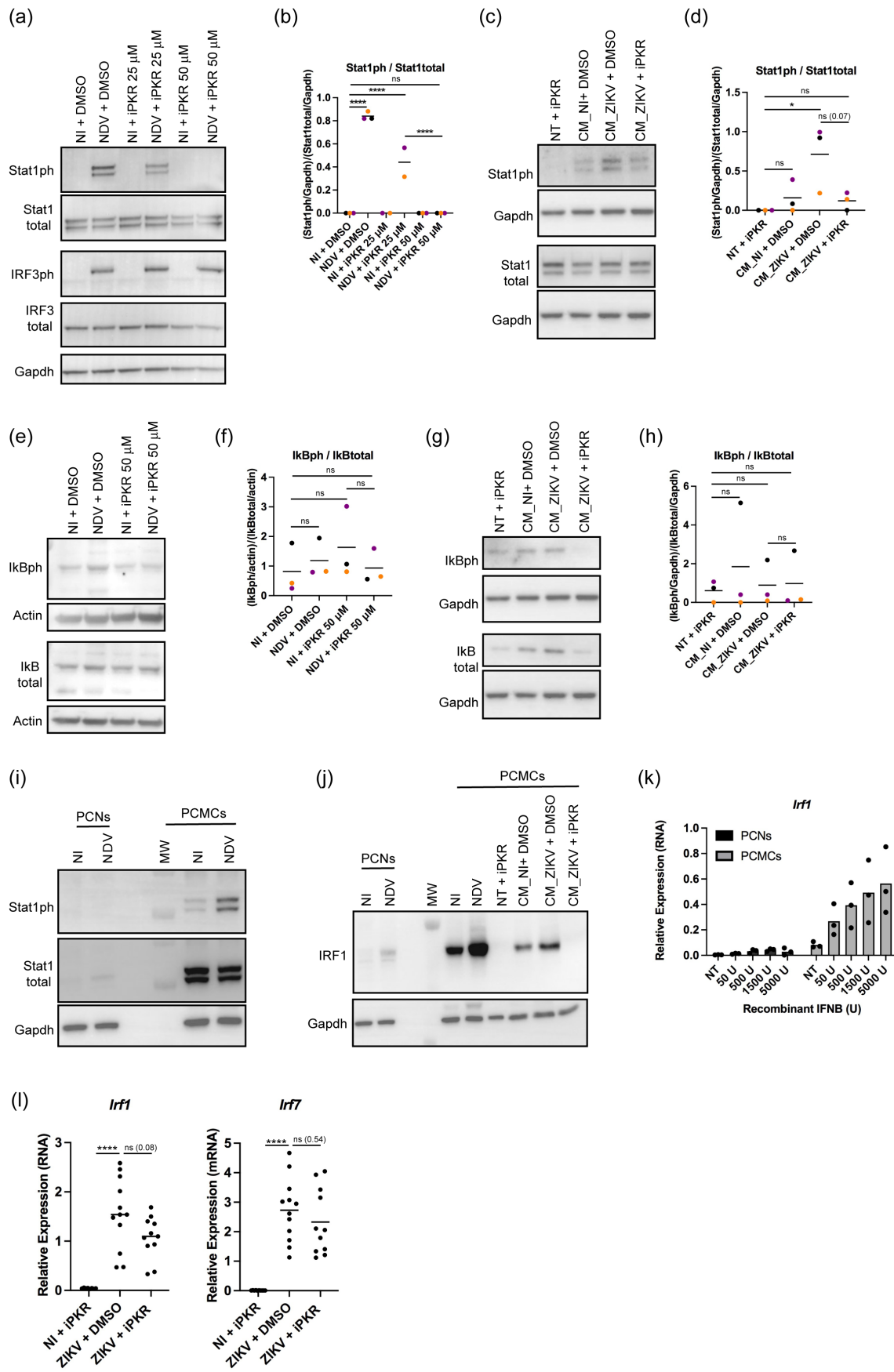


FIGURE 9 Legend on next page.

mechanism (Figure 10). First, IFNs-I secreted by ZIKV-infected neurons induce an IFNAR-dependent phosphorylation of STAT1 and STAT2 that triggers the expression of ISGs, leading to the up-regulation of PKR. Second, PKR induced by IFNs-I further increases STAT1 phosphorylation enhancing IRF1 expression, thereby maximizing the IRF1-dependent activation of the phagocytosis and pro-inflammatory response of NI microglial cells. Results presented here are consistent with previous works that have associated PKR with the regulation of neuroinflammation (Carret-Rebillat et al., 2015; Couturier et al., 2011) and more recently, to microglia activation and memory loss in a murine model of Gulf War Illness (Carreras et al., 2023). The major inhibitory effect of iPKR on STAT1 phosphorylation also explains the strong inhibition of ISGs expression in NDV-infected microglia treated with iPKR although *Ifnb1* gene expression remained significantly induced due to the presence of phosphorylated IRF3 that was not affected by iPKR. Results obtained here also point out a role for PKR in up-regulating the expression of the *Ifnb1* gene in microglial cells either treated with conditioned media from ZIKV-infected neurons (Figure 4b) or infected with NDV (Figure 8f). The PKR-dependent regulation of the expression of *Ifnb1* is likely mediated by IRF1 (Figure 10), which has been shown to bind the promoter region and induce the expression of *Ifnb1* (Feng et al., 2021). Further experiments are required to determine the mechanism behind PKR-driven phagocytosis. The gene *Cd11b* codes for one of the subunits of the receptor of C3 that is engaged in phagocytosis by microglia. We show here results indicative of an increase of *Cd11b* expression in vitro, following treatment of microglia with conditioned media from ZIKV-infected neurons (Figure 4c) and in vivo, following IC ZIKV infection (Figure S5). However, we did not detect a role for PKR in regulating ZIKV-induced *Cd11b* expression, which we also show not to be affected by recIFNB (Figure S7b). These results seem to exclude a role for PKR in regulating microglia's phagocytosis through *Cd11b* expression. However, CD11B needs to go through conformational changes in order to be functionally activated and we cannot exclude a role for PKR in this step. PKR could also affect microglia's phagocytosis by regulating microglia's ISG expression, which we show here to be strongly dependent on PKR.

Contrary to what we observed in microglia, PKR played no significant role in regulating the expression of genes associated with the IFN-I or pro-inflammatory response in neurons that express very low levels of STAT1 and IRF1. In vivo, in the brain of ZIKV-infected mice at 6 dpi, iPKR had non-significant effects on the level of expression of

the *Ifnb1* gene, of ISGs *Ifn4*, *Irf7*, *Isg15*, and on ZIKV RNA content. This is indicative of neurons being the main cells producing IFNs-I following brain ZIKV infection of adult immunocompetent mice under conditions where neurons are the only cell type infected by ZIKV (Figueiredo et al., 2019; Hayashida et al., 2019; Manet et al., 2022). Notwithstanding a lack of significant effect on IFNs-I expression in whole brain extracts, a significant inhibition of the expression of genes associated with the pro-inflammatory response induced following ZIKV infection was observed after iPKR treatment in vivo. It occurred concomitantly with a significant inhibition of the expression of the *Aif1* gene, of the increased cell body area of microglia and of the expression of *Irf1* induced by ZIKV-infection. This is indicative of PKR playing a critical role in regulating the reactivity of microglia in the brain of ZIKV-infected adult immunocompetent mice.

Although significant, the effect of iPKR treatment on the expression of genes associated with a pro-inflammatory response induced following ZIKV brain infection was not total and the effect on *Irf1* expression was only nearly significant suggesting the contribution of a mechanism independent of PKR. Such a mechanism could depend on the expression of IFNG that, through binding to its receptor IFNGR, is a major inducer of pSTAT1 and *Irf1* expression independently of the IFN-I response (Feng et al., 2021). Indeed, a significant increase of the expression of the *Ifnb1* gene coding for IFNG was observed after IC ZIKV infection at 6 dpi (Figure S5). Interestingly, the ZIKV-induced expression of *Ifnb1* was significantly inhibited by iPKR, possibly in relation with the effect of iPKR on the expression of genes coding for chemoattractants such as *Ccl2*, *Ccl5*, and *Cxcl10* that would limit the recruitment of IFNG-expressing cells. Even though this reflects the capacity of iPKR to limit the IFNG response in ZIKV-infected brains, a low level of *Ifnb1* expression could still be measured in the brain of iPKR-treated mice (Figure S5). This residual *Ifnb1* expression could be responsible for the residual iPKR-independent expression of *Irf1* and its subsequent effects on the pro-inflammatory response and phagocytic capacity of microglia.

Protective as well as deleterious functions have been associated with reactive microglia in the context of neurodegenerative diseases (AD) and viral infection (West Nile Virus, WNV). Although microglial cells participate in the clearance of A β plaques and are associated with a protective function in AD, there is also evidence that at later stages of the disease they mediate synapse loss, exacerbate Tau pathology and secrete neurotoxic factors (Hansen et al., 2018; Perea et al., 2020). In the case of WNV infection, microglia are crucial for limiting viral

FIGURE 9 Kinase PKR is a main regulator of the phosphorylation of STAT1 and of IRF1 expression in microglial cells. (a–h, j) Primary cultured microglial cells (PCMCs) were incubated with DMSO or the inhibitor of PKR (C16) for 1 h before being (a, e) either non- (NI) or NDV-infected and (c, g, j) either non-treated (NT) or treated with conditioned media from non- (CM_NI) or ZIKV-infected (CM_ZIKV) primary cultured neurons. Total protein extracts were collected 5 h after NDV infection and 6 h after treatment with CMs and submitted to a Western blot analysis. (b, d, f, h) Dot plots show means with one dot for each independent experiment represented in different colors. Significance was assessed by one-way ANOVA Tukey's multiple comparison test. p -value <0.0001 (****), <0.05 (*), and ns = not significant. (i–k) Primary cultured neurons (PCNs) and microglial cells (PCMCs) were (i, j) either non- (NI) or NDV-infected for 5 h or (k) treated with recombinant IFNB for 6 h. (i, j) Protein extracts or (k) RNAs were collected and submitted to Western blot or qPCR analysis respectively. (l) The level of expression of the *Irf1* and *Irf7* genes in total RNAs purified from whole brain extracts of mice described in Figure 6 was analyzed by RT-qPCR with respect to *Hrpt1* used as reference gene. Symbols represent individual mice with $n = 10$ (NI + iPKR), $n = 12$ (ZIKV + DMSO), and $n = 11$ (ZIKV + iPKR). Dot plots show means with significance assessed by one-way ANOVA Tukey's multiple comparison test. p -value <0.0001 (****) and ns = not significant.

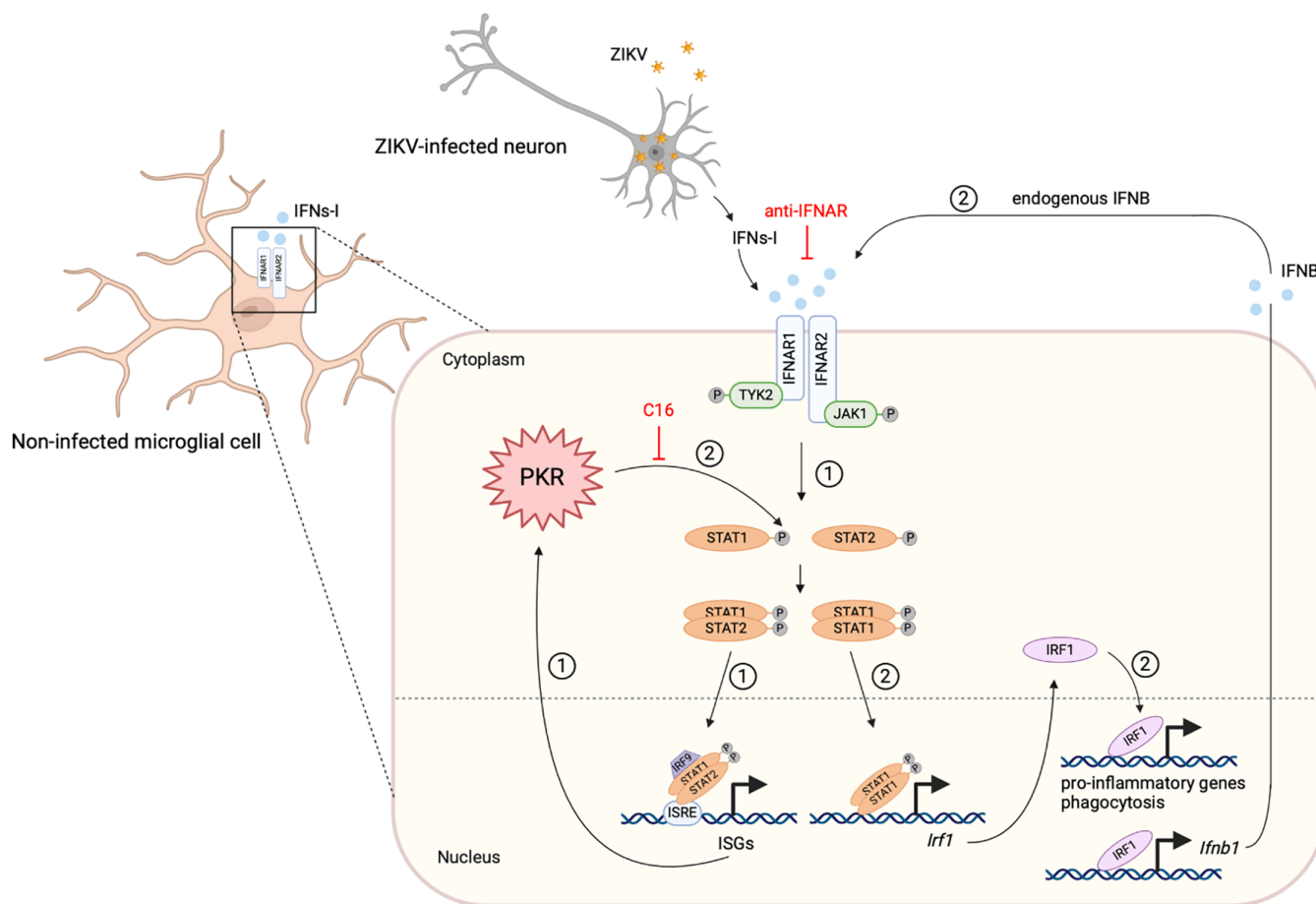


FIGURE 10 Type I IFNs secreted by ZIKV-infected neurons activate non-infected microglial cells through kinase PKR that up-regulates STAT1 phosphorylation and IRF1 expression. First, type I IFNs secreted by ZIKV-infected neurons bind to the IFNAR receptor of non-infected microglial cells to induce the phosphorylation of STAT1 and STAT2 necessary to activate the expression of ISGs among which the gene coding for kinase PKR (Schneider et al., 2014). Second, kinase PKR increases the rate of phosphorylation of STAT1 in microglial cells followed by the subsequent increase of the expression of the gene coding for transcription factor IRF1 that activates the pro-inflammatory response and the phagocytic capacity of microglial cells (Gao et al., 2019; Yang et al., 2022) alongside with inducing the expression of the *Ifnb1* gene coding for IFNB (Feng et al., 2021). The diagram was created using BioRender.com.

spread but they are also responsible for functional synapse loss, cognitive impairment and neurodegeneration (Vittor et al., 2020). Thus, while proper microglia function can be protective and crucial for pathogen host defense, its prolonged activation can be deleterious and lead to neuronal injury. In the case ZIKV infection, a loss of neurons has been reported following neonatal infection of immunocompetent mice (Ireland et al., 2020) but this was not reported by Figueiredo et al. (2019) while infecting adult mice, even though they observed functional synapse loss and memory impairment (Figueiredo et al., 2019). Future work using partial microglia depletion and long-term PKR inhibition should help us to determine the positive and negative functional implications of the PKR-dependent ZIKV-induced activation of microglia with respect to ZIKV replication, ZIKV-induced inflammatory and DAM response, neuronal and synapse loss and Tau pathology spreading.

Kinase PKR is a major antiviral factor that is targeted by several viruses (Dabo & Meurs, 2012; Rothenburg & Brennan, 2020) but, on the contrary, ZIKV has been shown to take advantage of PKR activity to

favor its replication in vitro, in human dermal fibroblasts (Ponia et al., 2021) and A549 cells (Ricciardi-Jorge et al., 2023). However, there is presently no data demonstrating that this could also be the case in vivo, in neuronal cells. Under conditions used here, we did not observe an effect of PKR inhibition, positive or negative, on ZIKV replication in the brain of ZIKV-infected adult mice (Figure 6c). This rules out the possibility that the effects of iPKR treatment on ZIKV-induced pro-inflammatory response could be the consequence of an effect on ZIKV replication. Hence, inhibiting PKR activity appears as a way to dampen ZIKV-induced brain inflammation without promoting viral replication.

Beyond viral infection, the expression of IFNs-I can be induced by self-nucleic acids resulting from, among others, an excess of DNA damage, the activation of endogenous retroelements or mitochondria dysfunction (Crow & Stetson, 2022; Kato et al., 2017; Rongvaux, 2018; Stetson et al., 2008; Wolf et al., 2016; Zhao et al., 2018). Results obtained in this work, suggest that the persistent production of IFNs-I by aged/stressed/damaged neurons could induce a persistent activation of "naïve" microglia and thus account for the presence of subsets

of active microglial cells displaying an IFN-I response signature that have been described in association with aging (Deczkowska et al., 2017; Lopes et al., 2022; Olah et al., 2018; Sala Frigerio et al., 2019), neuropathologies such as AD (Chen & Colonna, 2021; Ising et al., 2019; Mathys et al., 2017; Olah et al., 2020; Sala Frigerio et al., 2019) and brain injury (Todd et al., 2023). It would be interesting to analyze if, as demonstrated in this work, a PKR-dependent phosphorylation of STAT1 leading to an increased expression of IRF1 is also at work in these neuropathologies associated with an Interferon Responsive Microglia (IRM) signature.

AUTHOR CONTRIBUTIONS

EB conceived and supervised this study. VB and ZM designed and performed most of the experiments and analyzed data. LC, GC, FL, JP MO, HS, MS, and RM performed experiments. SS, FN, and LB provided conceptual advice. EB, XM, and MCG designed experiments and analyzed data. EB wrote the paper. All authors commented on and edited the manuscript.

ACKNOWLEDGMENTS

This work was supported by the following grants: Agence Nationale de la Recherche (ANR) NeuroZika (ANR-20-CE16-0017) and the French Government's Investissement d'Avenir program, Laboratoire d'Excellence: IBEID (Integrative Biology of Emerging Infectious Diseases, ANR-10-LABX-62-IBEID) and DISTALZ (Development of Innovative Strategies for a Transdisciplinary approach to Alzheimer's disease) as well as grants from CNRS, Inserm and Université Paris Cité to Florence Niedergang. We are grateful to the Virology Laboratory of the Institut Pasteur of French Guyana (National Reference Center for Arboviruses) for providing the FG15 ZIKV strain. We thank Maryline Favier and Rachel Onifarasoaniaina from the HistIM facility and Gabriel LeGoff from the IMAG'IC facility of Institut Cochin that is part of the national France-BioImaging infrastructure supported by the ANR-10_INBS-04 grant.

CONFLICT OF INTEREST STATEMENT

The authors declare no conflicts of interest.

DATA AVAILABILITY STATEMENT

The data that support the findings of this study are available from the corresponding author upon reasonable request.

ORCID

Xavier Montagutelli  <https://orcid.org/0000-0002-9372-5398>

Eliette Bonnefoy  <https://orcid.org/0000-0002-9534-2104>

REFERENCES

- Acosta-Ampudia, Y., Monsalve, D. M., Castillo-Medina, L. F., Rodríguez, Y., Pacheco, Y., Halstead, S., Willison, H. J., Anaya, J. M., & Ramírez-Santana, C. (2018). Autoimmune neurological conditions associated with Zika virus infection. *Frontiers in Molecular Neuroscience*, 11, 116. <https://doi.org/10.3389/fnmol.2018.00116>
- Arutyunov, A., Durán-Laforet, V., Ai, S., Ferrari, L., Murphy, R., Schafer, D. P., & Klein, R. S. (2024). West Nile virus-induced expression of senescent gene *Lgals3bp* regulates microglial phenotype within cerebral cortex. *Biomolecules*, 14(7), 808. <https://doi.org/10.3390/biom14070808>
- Arutyunov, A., & Klein, R. S. (2023). Microglia at the scene of the crime: What their transcriptomics reveal about brain health. *Current Opinion in Neurology*, 36(3), 207–213. <https://doi.org/10.1097/WCO.0000000000001151>
- Baruch, K., Deczkowska, A., David, E., Castellano, J. M., Miller, O., Kertser, A., Berkutzi, T., Barnett-Itzhaki, Z., Bezalel, D., Wyss-Coray, T., Amit, I., & Schwartz, M. (2014). Aging. Aging-induced type I interferon response at the choroid plexus negatively affects brain function. *Science*, 346(6205), 89–93. <https://doi.org/10.1126/science.1252945>
- Borst, K., Dumas, A. A., & Prinz, M. (2021). Microglia: Immune and non-immune functions. *Immunity*, 54(10), 2194–2208. <https://doi.org/10.1016/j.immuni.2021.09.014>
- Bourdon, M., Manet, C., Conquet, L., Ramaugé Parra, C., Kornobis, E., Bonnefoy, E., & Montagutelli, X. (2023). Susceptibility to Zika virus in a collaborative cross mouse strain is induced by Irf3 deficiency in vitro but requires other variants in vivo. *PLoS Pathogens*, 19(9), e1011446. <https://doi.org/10.1371/journal.ppat.1011446>
- Butler, C. A., Popescu, A. S., Kitchener, E. J. A., Allendorf, D. H., Puigdemívol, M., & Brown, G. C. (2021). Microglial phagocytosis of neurons in neurodegeneration, and its regulation. *Journal of Neurochemistry*, 158(3), 621–639. <https://doi.org/10.1111/jnc.15327>
- Butovsky, O., & Weiner, H. L. (2018). Microglial signatures and their role in health and disease. *Nature Reviews Neuroscience*, 19(10), 622–635. <https://doi.org/10.1038/s41583-018-0057-5>
- Butturini, E., Boriero, D., Carcereri de Prati, A., & Mariotto, S. (2019). STAT1 drives M1 microglia activation and neuroinflammation under hypoxia. *Archives of Biochemistry and Biophysics*, 669, 22–30. <https://doi.org/10.1016/j.abb.2019.05.011>
- Carreras, I., Jung, Y., Lopez-Benitez, J., Tognoni, C. M., & Dedeoglu, A. (2023). Fingolimod mitigates memory loss in a mouse model of gulf war illness amid decreasing the activation of microglia, protein kinase R, and NFκB. *Neurotoxicology*, 96, 197–206. <https://doi.org/10.1016/j.neuro.2023.05.006>
- Carret-Rebillat, A. S., Pace, C., Gourmaud, S., Ravasi, L., Montagne-Stora, S., Longueville, S., Tible, M., Sudol, E., Chang, R. C., Paquet, C., Mouton-Liger, F., & Hugon, J. (2015). Neuroinflammation and Aβ accumulation linked to systemic inflammation are decreased by genetic PKR down-regulation. *Scientific Reports*, 5, 8489. <https://doi.org/10.1038/srep08489>
- Chen, Y., & Colonna, M. (2021). Microglia in Alzheimer's disease at single-cell level. Are there common patterns in humans and mice? *The Journal of Experimental Medicine*, 218(9), e20202717. <https://doi.org/10.1084/jem.20202717>
- Chhatbar, C., & Prinz, M. (2021). The roles of microglia in viral encephalitis: From sensome to therapeutic targeting. *Cellular & Molecular Immunology*, 18(2), 250–258. <https://doi.org/10.1038/s41423-020-00620-5>
- Christian, K. M., Song, H., & Ming, G. L. (2019). Pathophysiology and mechanisms of Zika virus infection in the nervous system. *Annual Review of Neuroscience*, 42, 249–269. <https://doi.org/10.1146/annurev-neuro-080317-062231>
- Couturier, J., Paccalin, M., Morel, M., Terro, F., Milin, S., Pontcharraud, R., Fauconneau, B., & Page, G. (2011). Prevention of the β-amyloid peptide-induced inflammatory process by inhibition of double-stranded RNA-dependent protein kinase in primary murine mixed cocultures. *Journal of Neuroinflammation*, 8, 72. <https://doi.org/10.1186/1742-2094-8-72>
- Crow, Y. J., & Manel, N. (2015). Aicardi-Goutières syndrome and the type I interferonopathies. *Nature Reviews Immunology*, 15(7), 429–440. <https://doi.org/10.1038/nri3850>
- Crow, Y. J., & Stetson, D. B. (2022). The type I interferonopathies: 10 years on. *Nature Reviews Immunology*, 22(8), 471–483. <https://doi.org/10.1038/s41577-021-00633-9>

- da Silva, I. R. F., Frontera, J. A., Bispo de Filippis, A. M., Nascimento, O. J. M. D., & RIO-GBS-ZIKV Research Group. (2017). Neurologic complications associated with the Zika virus in Brazilian adults. *JAMA Neurology*, 74(10), 1190–1198. <https://doi.org/10.1001/jamaneurol.2017.1703>
- Dabo, S., & Meurs, E. F. (2012). dsRNA-dependent protein kinase PKR and its role in stress, signaling and HCV infection. *Viruses*, 4(11), 2598–2635. <https://doi.org/10.3390/v4112598>
- Damisah, E. C., Hill, R. A., Rai, A., Chen, F., Rothlin, C. V., Ghosh, S., & Grutzendler, J. (2020). Astrocytes and microglia play orchestrated roles and respect phagocytic territories during neuronal corpse removal in vivo. *Science Advances*, 6(26), eaba3239. <https://doi.org/10.1126/sciadv.aba3239>
- de Oliveira Souza, N. I., Frost, P. S., França, J. V., Nascimento-Viana, J. B., Neris, R. L. S., Freitas, L., Pinheiro, D. J. L. L., Nogueira, C. O., Neves, G., Chimelli, L., De Felice, F. G., Cavalheiro, É. A., Ferreira, S. T., Assunção-Miranda, I., Figueiredo, C. P., Da Poian, A. T., & Clarke, J. R. (2018). Acute and chronic neurological consequences of early-life Zika virus infection in mice. *Science Translational Medicine*, 10(444), eaar2749. <https://doi.org/10.1126/scitransmed.aar2749>
- Deczkowska, A., Matcovitch-Natan, O., Tzitsou-Kampeli, A., Ben-Hamo, S., Dvir-Szternfeld, R., Spinrad, A., Singer, O., David, E., Winter, D. R., Smith, L. K., Kertser, A., Baruch, K., Rosenzweig, N., Terem, A., Prinz, M., Villeda, S., Citri, A., Amit, I., & Schwartz, M. (2017). Mef2C restrains microglial inflammatory response and is lost in brain ageing in an IFN-I-dependent manner. *Nature Communications*, 8(1), 717. <https://doi.org/10.1038/s41467-017-00769-0>
- Feng, H., Zhang, Y. B., Gui, J. F., Lemon, S. M., & Yamane, D. (2021). Interferon regulatory factor 1 (IRF1) and anti-pathogen innate immune responses. *PLoS Pathogens*, 17(1), e1009220. <https://doi.org/10.1371/journal.ppat.1009220>
- Figueiredo, C. P., Barros-Aragão, F. G. Q., Neris, R. L. S., Frost, P. S., Soares, C., Souza, I. N. O., Zeidler, J. D., Zamberlan, D. C., de Sousa, V. L., Souza, A. S., Guimarães, A. L. A., Bellio, M., Marcondes de Souza, J., Alves-Leon, S. V., Neves, G. A., Paula-Neto, H. A., Castro, N. G., De Felice, F. G., Assunção-Miranda, I., ... Ferreira, S. T. (2019). Zika virus replicates in adult human brain tissue and impairs synapses and memory in mice. *Nature Communications*, 10(1), 3890. <https://doi.org/10.1038/s41467-019-11866-7>
- Forero, A., Ozarkar, S., Li, H., Lee, C. H., Hemann, E. A., Nadjombati, M. S., Hendricks, M. R., So, L., Green, R., Roy, C. N., Sarkar, S. N., von Moltke, J., Anderson, S. K., Gale, M., Jr, & Savan, R. (2019). Differential Activation of the Transcription Factor IRF1 Underlies the Distinct Immune Responses Elicited by Type I and Type III Interferons. *Immunity*, 51(3), 451–464.e6. <https://doi.org/10.1016/j.immuni.2019.07.007>
- Gal-Ben-Ari, S., Barrera, I., Ehrlich, M., & Rosenblum, K. (2019). PKR: A kinase to remember. *Frontiers in Molecular Neuroscience*, 11, 480. <https://doi.org/10.3389/fnmol.2018.00480>
- Gao, T., Jernigan, J., Raza, S. A., Dammer, E. B., Xiao, H., Seyfried, N. T., Levey, A. I., & Rangaraju, S. (2019). Transcriptional regulation of homeostatic and disease-associated-microglial genes by IRF1, LXR β , and CEBP α . *Glia*, 67(10), 1958–1975. <https://doi.org/10.1002/glia.23678>
- Garaschuk, O., & Verkhratsky, A. (2019). Physiology of microglia. *Methods in Molecular Biology*, 2034: 27–40. https://doi.org/10.1007/978-1-4939-9658-2_3
- Grabert, K., Michoel, T., Karavolos, M. H., Clohisey, S., Baillie, J. K., Stevens, M. P., Freeman, T. C., Summers, K. M., & McColl, B. W. (2016). Microglial brain region-dependent diversity and selective regional sensitivities to aging. *Nature Neuroscience*, 19(3), 504–516. <https://doi.org/10.1038/nn.4222>
- Hansen, D. V., Hanson, J. E., & Sheng, M. (2018). Microglia in Alzheimer's disease. *Journal of Cell Biology*, 217(2), 459–472. <https://doi.org/10.1083/jcb.201709069>
- Hayashida, E., Ling, Z. L., Ashhurst, T. M., Viengkhou, B., Jung, S. R., Songkhunawej, P., West, P. K., King, N. J. C., & Hofer, M. J. (2019). Zika virus encephalitis in immunocompetent mice is dominated by innate immune cells and does not require T or B cells. *Journal of Neuroinflammation*, 16(1), 177. <https://doi.org/10.1186/s12974-019-1566-5>
- Hofer, M. J., & Campbell, I. L. (2013). Type I interferon in neurological disease—the devil from within. *Cytokine & Growth Factor Reviews*, 24(3), 257–267. <https://doi.org/10.1016/j.cytogfr.2013.03.006>
- Hong, S., Beja-Glasser, V. F., Nfonoyim, B. M., Frouin, A., Li, S., Ramakrishnan, S., Merry, K. M., Shi, Q., Rosenthal, A., Barres, B. A., Lemere, C. A., Selkoe, D. J., & Stevens, B. (2016). Complement and microglia mediate early synapse loss in Alzheimer mouse models. *Science*, 352(6286), 712–716. <https://doi.org/10.1126/science.aad8373>
- Hsu, D. C., Chumpolkulwong, K., Corley, M. J., Hunsawong, T., Inthawong, D., Schuetz, A., Imerbsin, R., Silson, D., Nadee, P., Sopanaporn, J., Phuang-Ngern, Y., Klungthong, C., Reed, M., Fernandez, S., Ndhlovu, L. C., Paul, R., Lugo-Roman, L., Michael, N. L., Modjarrad, K., ... Vasani, S. (2022). Neurocognitive impact of Zika virus infection in adult rhesus macaques. *Journal of Neuroinflammation*, 19(1), 40. <https://doi.org/10.1186/s12974-022-02402-4>
- Ireland, D. D. C., Manangeeswaran, M., Lewkowicz, A. P., Engel, K., Clark, S. M., Laniyan, A., Sykes, J., Lee, H. N., McWilliams, I. L., Kelley-Baker, L., Tonelli, L. H., & Verthelyi, D. (2020). Long-term persistence of infectious Zika virus: Inflammation and behavioral sequela in mice. *PLoS Pathogens*, 16(12), e1008689. <https://doi.org/10.1371/journal.ppat.1008689>
- Ising, C., Venegas, C., Zhang, S., Scheiblich, H., Schmidt, S. V., Vieira-Saecker, A., Schwartz, S., Albasset, S., McManus, R. M., Tejera, D., Griep, A., Santarelli, F., Brosseon, F., Opitz, S., Stunden, J., Merten, M., Kaye, R., Golenbock, D. T., Blum, D., ... Heneka, M. T. (2019). NLRP3 inflammasome activation drives tau pathology. *Nature*, 575(7784), 669–673. <https://doi.org/10.1038/s41586-019-1769-z>
- Javed, F., Manzoor, K. N., Ali, M., Haq, I. U., Khan, A. A., Zaib, A., & Manzoor, S. (2018). Zika virus: What we need to know? *Journal of Basic Microbiology*, 58(1), 3–16. <https://doi.org/10.1002/jobm.201700398>
- Jensen, S., & Thomsen, A. R. (2012). Sensing of RNA viruses: A review of innate immune receptors involved in recognizing RNA virus invasion. *Journal of Virology*, 86(6), 2900–2910. <https://doi.org/10.1128/JVI.05738-11>
- Ji, R. R., Berta, T., & Nedergaard, M. (2013). Glia and pain: Is chronic pain a gliopathy? *Pain*, 154(1), S10–S28. <https://doi.org/10.1016/j.pain.2013.06.022>
- Kato, K., Omura, H., Ishitani, R., & Nureki, O. (2017). Cyclic GMP-AMP as an endogenous second messenger in innate immune signaling by cytosolic DNA. *Annual Review of Biochemistry*, 86, 541–566. <https://doi.org/10.1146/annurev-biochem-061516-044813>
- Keren-Shaul, H., Spinrad, A., Weiner, A., Matcovitch-Natan, O., Dvir-Szternfeld, R., Ulland, T. K., David, E., Baruch, K., Lara-Astaiso, D., Toth, B., Itzkovitz, S., Colonna, M., Schwartz, M., & Amit, I. (2017). A unique microglia type associated with restricting development of Alzheimer's disease. *Cell*, 169(7), 1276–1290.e17. <https://doi.org/10.1016/j.cell.2017.05.018>
- Lannuzel, A., Fergé, J. L., Lobjois, Q., Signate, A., Rozé, B., Tressières, B., Madec, Y., Poullain, P., Herrmann, C., Najjoulah, F., McGovern, E., Savidan, A. C., Valentino, R., Breurec, S., Césaire, R., Hirsch, E., Lledo, P. M., Thiery, G., Cabié, A., ... Roze, E. (2019). Long-term outcome in neuroZika: When biological diagnosis matters. *Neurology*, 92(21), e2406–e2420. <https://doi.org/10.1212/WNL.0000000000007536>
- Lopes, K. P., Snijders, G. J. L., Humphrey, J., Allan, A., Sneboer, M. A. M., Navarro, E., Schilder, B. M., Vialle, R. A., Parks, M., Missall, R., van Zuiden, W., Gigase, F. A. J., Kübler, R., van Berlekom, A. B., Hicks, E. M., Böttcher, C., Priller, J., Kahn, R. S., de Witte, L. D., & Raj, T. (2022). Genetic analysis of the human microglial transcriptome



- across brain regions, aging and disease pathologies. *Nature Genetics*, 54(1), 4–17. <https://doi.org/10.1038/s41588-021-00976-y>
- Manet, C., Mansuroglu, Z., Conquet, L., Bortolin, V., Comptdaer, T., Segre, H., Bourdon, M., Menidjel, R., Stadler, N., Tian, G., Herit, F., Niedergang, F., Souès, S., Buée, L., Galas, M. C., Montagutelli, X., & Bonnefoy, E. (2022). Zika virus infection of mature neurons from immunocompetent mice generates a disease-associated microglia and a tauopathy-like phenotype in link with a delayed interferon beta response. *Journal of Neuroinflammation*, 19(1), 307. <https://doi.org/10.1186/s12974-022-02668-8>
- Manet, C., Simon-Lorière, E., Jouvion, G., Hardy, D., Prot, M., Conquet, L., Flamand, M., Panthier, J. J., Sakuntabhai, A., & Montagutelli, X. (2020). Genetic diversity of collaborative cross mice controls viral replication, clinical severity, and brain pathology induced by Zika virus infection, independently of *Oas1b*. *Journal of Virology*, 94(3), e01034. <https://doi.org/10.1128/JVI.01034-19>
- Mathys, H., Adakkan, C., Gao, F., Young, J. Z., Manet, E., Hemberg, M., De Jager, P. L., Ransohoff, R. M., Regev, A., & Tsai, L. H. (2017). Temporal tracking of microglia activation in neurodegeneration at single-cell resolution. *Cell Reports*, 21(2), 366–380. <https://doi.org/10.1016/j.celrep.2017.09.039>
- Nayak, D., Johnson, K. R., Heydari, S., Roth, T. L., Zinselmeyer, B. H., & McGavern, D. B. (2013). Type I interferon programs innate myeloid dynamics and gene expression in the virally infected nervous system. *PLoS Pathogens*, 9(5), e1003395. <https://doi.org/10.1371/journal.ppat.1003395>
- Nazmi, A., Field, R. H., Griffin, E. W., Haugh, O., Hennessy, E., Cox, D., Reis, R., Tortorelli, L., Murray, C. L., Lopez-Rodriguez, A. B., Jin, L., Lavelle, E. C., Dunne, A., & Cunningham, C. (2019). Chronic neurodegeneration induces type I interferon synthesis via STING, shaping microglial phenotype and accelerating disease progression. *Glia*, 67(7), 1254–1276. <https://doi.org/10.1002/glia.23592>
- Neumann, H., Kotter, M. R., & Franklin, R. J. (2009). Debris clearance by microglia: An essential link between degeneration and regeneration. *Brain: A Journal of Neurology*, 132(Pt 2), 288–295. <https://doi.org/10.1093/brain/awn109>
- Olah, M., Menon, V., Habib, N., Taga, M. F., Ma, Y., Yung, C. J., Cimpean, M., Khairallah, A., Coronas-Samano, G., Sankowski, R., Grün, D., Kroshilina, A. A., Dionne, D., Sarkis, R. A., Cosgrove, G. R., Helgager, J., Golden, J. A., Pennell, P. B., Prinz, M., ... De Jager, P. L. (2020). Single cell RNA sequencing of human microglia uncovers a subset associated with Alzheimer's disease. *Nature Communications*, 11(1), 6129. <https://doi.org/10.1038/s41467-020-19737-2>
- Olah, M., Patrick, E., Villani, A. C., Xu, J., White, C. C., Ryan, K. J., Piehowski, P., Kapasi, A., Nejad, P., Cimpean, M., Connor, S., Yung, C. J., Frangieh, M., McHenry, A., Elyaman, W., Petyuk, V., Schneider, J. A., Bennett, D. A., De Jager, P. L., & Bradshaw, E. M. (2018). A transcriptomic atlas of aged human microglia. *Nature Communications*, 9(1), 539. <https://doi.org/10.1038/s41467-018-02926-5>
- Paolicelli, R. C., Sierra, A., Stevens, B., Tremblay, M. E., Aguzzi, A., Ajami, B., Amit, I., Audinat, E., Bechmann, I., Bennett, M., Bennett, F., Bessis, A., Biber, K., Bilbo, S., Blurton-Jones, M., Boddeke, E., Brites, D., Brône, B., Brown, G. C., ... Wyss-Coray, T. (2022). Microglia states and nomenclature: A field at its crossroads. *Neuron*, 110(21), 3458–3483. <https://doi.org/10.1016/j.neuron.2022.10.020>
- Perea, J. R., Bolós, M., & Avila, J. (2020). Microglia in Alzheimer's disease in the context of tau pathology. *Biomolecules*, 10(10), 1439. <https://doi.org/10.3390/biom10101439>
- Pham, A. M., Santa Maria, F. G., Lahiri, T., Friedman, E., Marié, I. J., & Levy, D. E. (2016). PKR Transduces MDA5-Dependent Signals for Type I IFN Induction. *PLoS pathogens*, 12(3), e1005489. <https://doi.org.proxy.insermbiblio.inist.fr/10.1371/journal.ppat.1005489>
- Ponia, S. S., Robertson, S. J., McNally, K. L., Subramanian, G., Sturdevant, G. L., Lewis, M., Jessop, F., Kendall, C., Gallegos, D., Hay, A., Schwartz, C., Rosenke, R., Saturday, G., Bosio, C. M., Martens, C., & Best, S. M. (2021). Mitophagy antagonism by ZIKV reveals Ajuba as a regulator of PINK1 signaling, PKR-dependent inflammation, and viral invasion of tissues. *Cell Reports*, 37(4), 109888. <https://doi.org/10.1016/j.celrep.2021.109888>
- Rangaraju, S., Dammer, E. B., Raza, S. A., Rathakrishnan, P., Xiao, H., Gao, T., Duong, D. M., Pennington, M. W., Lah, J. J., Seyfried, N. T., & Levey, A. I. (2018). Identification and therapeutic modulation of a pro-inflammatory subset of disease-associated-microglia in Alzheimer's disease. *Molecular Neurodegeneration*, 13(1), 24. <https://doi.org/10.1186/s13024-018-0254-8>
- Ransohoff, R. M., & El Khoury, J. (2015). Microglia in health and disease. *Cold Spring Harbor Perspectives in Biology*, 8(1), a020560. <https://doi.org/10.1101/cshperspect.a020560>
- Raper, J., Kovacs-Balint, Z., Mavigner, M., Gumber, S., Burke, M. W., Habib, J., Mattingly, C., Fair, D., Earl, E., Feczko, E., Styner, M., Jean, S. M., Cohen, J. K., Suthar, M. S., Sanchez, M. M., Alvarado, M. C., & Chahroudi, A. (2020). Long-term alterations in brain and behavior after postnatal Zika virus infection in infant macaques. *Nature Communications*, 11(1), 2534. <https://doi.org/10.1038/s41467-020-16320-7>
- Ricciardi-Jorge, T., da Rocha, E. L., Gonzalez-Kozlova, E., Rodrigues-Luiz, G. F., Ferguson, B. J., Sweeney, T., Irigoyen, N., & Mansur, D. S. (2023). PKR-mediated stress response enhances dengue and Zika virus replication. *MBio*, 14(5), e0093423. <https://doi.org/10.1128/mbio.00934-23>
- Rongvaux, A. (2018). Innate immunity and tolerance toward mitochondria. *Mitochondrion*, 41, 14–20. <https://doi.org/10.1016/j.mito.2017.10.007>
- Rothenburg, S., & Brennan, G. (2020). Species-specific host-virus interactions: Implications for viral host range and virulence. *Trends in Microbiology*, 28(1), 46–56. <https://doi.org/10.1016/j.tim.2019.08.007>
- Roy, E. R., Chiu, G., Li, S., Propson, N. E., Kanchi, R., Wang, B., Coarfa, C., Zheng, H., & Cao, W. (2022). Concerted type I interferon signaling in microglia and neural cells promotes memory impairment associated with amyloid β plaques. *Immunity*, 55(5), 879–894.e6. <https://doi.org/10.1016/j.immuni.2022.03.018>
- Roy, E. R., Wang, B., Wan, Y. W., Chiu, G., Cole, A., Yin, Z., Propson, N. E., Xu, Y., Jankowsky, J. L., Liu, Z., Lee, V. M., Trojanowski, J. Q., Ginsberg, S. D., Butovsky, O., Zheng, H., & Cao, W. (2020). Type I interferon response drives neuroinflammation and synapse loss in Alzheimer disease. *The Journal of Clinical Investigation*, 130(4), 1912–1930. <https://doi.org/10.1172/JCI133737>
- Sala Frigerio, C., Wolfs, L., Fattorelli, N., Thrupp, N., Voytyuk, I., Schmidt, I., Mancuso, R., Chen, W. T., Woodbury, M. E., Srivastava, G., Möller, T., Hudry, E., Das, S., Saido, T., Karran, E., Hyman, B., Perry, V. H., Fiers, M., & De Strooper, B. (2019). The major risk factors for Alzheimer's disease: Age, sex, and genes modulate the microglia response to A β plaques. *Cell Reports*, 27(4), 1293–1306.e6. <https://doi.org/10.1016/j.celrep.2019.03.099>
- Savage, J. C., Carrier, M., & Tremblay, M. È. (2019). Morphology of microglia across contexts of health and disease. *Methods in Molecular Biology*, 2034, 13–26. https://doi.org/10.1007/978-1-4939-9658-2_2
- Schafer, D. P., Lehrman, E. K., Kautzman, A. G., Koyama, R., Mardinly, A. R., Yamasaki, R., Ransohoff, R. M., Greenberg, M. E., Barres, B. A., & Stevens, B. (2012). Microglia sculpt postnatal neural circuits in an activity and complement-dependent manner. *Neuron*, 74(4), 691–705. <https://doi.org/10.1016/j.neuron.2012.03.026>
- Schneider, W. M., Chevillotte, M. D., & Rice, C. M. (2014). Interferon-stimulated genes: A complex web of host defenses. *Annual Review of Immunology*, 32, 513–545. <https://doi.org/10.1146/annurev-immunol-032713-120231>
- Schwabenland, M., Brück, W., Priller, J., Stadelmann, C., Lassmann, H., & Prinz, M. (2021). Analyzing microglial phenotypes across neuropathologies: A practical guide. *Acta Neuropathologica*, 142(6), 923–936. <https://doi.org/10.1007/s00401-021-02370-8>

- Sheehan, K. C., Lai, K. S., Dunn, G. P., Bruce, A. T., Diamond, M. S., Heutel, J. D., Dungo-Arthur, C., Carrero, J. A., White, J. M., Hertzog, P. J., & Schreiber, R. D. (2006). Blocking monoclonal antibodies specific for mouse IFN- α /beta receptor subunit 1 (IFNAR-1) from mice immunized by in vivo hydrodynamic transfection. *Journal of Interferon & Cytokine Research*, 26(11), 804–819. <https://doi.org/10.1089/jir.2006.26.804>
- Stetson, D. B., Ko, J. S., Heidmann, T., & Medzhitov, R. (2008). Trex1 prevents cell-intrinsic initiation of autoimmunity. *Cell*, 134(4), 587–598. <https://doi.org/10.1016/j.cell.2008.06.032>
- Stevens, B., Allen, N. J., Vazquez, L. E., Howell, G. R., Christopherson, K. S., Nouri, N., Micheva, K. D., Mehalow, A. K., Huberman, A. D., Stafford, B., Sher, A., Litke, A. M., Lambris, J. D., Smith, S. J., John, S. W., & Barres, B. A. (2007). The classical complement cascade mediates CNS synapse elimination. *Cell*, 131(6), 1164–1178. <https://doi.org/10.1016/j.cell.2007.10.036>
- Taylor, J. M., Minter, M. R., Newman, A. G., Zhang, M., Adlard, P. A., & Crack, P. J. (2014). Type-1 interferon signaling mediates neuro-inflammatory events in models of Alzheimer's disease. *Neurobiology of Aging*, 35(5), 1012–1023. <https://doi.org/10.1016/j.neurobiolaging.2013.10.089>
- Todd, B. P., Luo, Z., Gilkes, N., Chimenti, M. S., Peterson, Z., Mix, M. R., Harty, J. T., Nickl-Jockschat, T., Ferguson, P. J., Bassuk, A. G., & Newell, E. A. (2023). Selective neuroimmune modulation by type I interferon drives neuropathology and neurologic dysfunction following traumatic brain injury. *Acta Neuropathologica Communications*, 11(1), 134. <https://doi.org/10.1186/s40478-023-01635-5>
- Vasek, M. J., Garber, C., Dorsey, D., Durrant, D. M., Bollman, B., Soung, A., Yu, J., Perez-Torres, C., Frouin, A., Wilton, D. K., Funk, K., DeMasters, B. K., Jiang, X., Bowen, J. R., Mennerick, S., Robinson, J. K., Garbow, J. R., Tyler, K. L., Suthar, M. S., ... Klein, R. S. (2016). A complement-microglial axis drives synapse loss during virus-induced memory impairment. *Nature*, 534(7608), 538–543. <https://doi.org/10.1038/nature18283>
- Villa, A., Gelosa, P., Castiglioni, L., Cimino, M., Rizzi, N., Pepe, G., Lolli, F., Marcello, E., Sironi, L., Vegeto, E., & Maggi, A. (2018). Sex-specific features of microglia from adult mice. *Cell Reports*, 23(12), 3501–3511. <https://doi.org/10.1016/j.celrep.2018.05.048>
- Violet, M., Chauderlier, A., Delattre, L., Tardivel, M., Chouala, M. S., Sultan, A., Marciniak, E., Humez, S., Binder, L., Kaye, R., Lefebvre, B., Bonnefoy, E., Buée, L., & Galas, M. C. (2015). Prefibrillar Tau oligomers alter the nucleic acid protective function of Tau in hippocampal neurons in vivo. *Neurobiology of Disease*, 82, 540–551. <https://doi-org.proxy.insermbiblio.inist.fr/10.1016/j.nbd.2015.09.003>
- Vittor, A. Y., Long, M., Chakrabarty, P., Aycok, L., Kollu, V., & DeKosky, S. T. (2020). West Nile virus-induced neurologic sequelae—relationship to neurodegenerative cascades and dementias. *Current Tropical Medicine Reports*, 7(1), 25–36. <https://doi.org/10.1007/s40475-020-00200-7>
- Wang, C., Yue, H., Hu, Z., Shen, Y., Ma, J., Li, J., Wang, X. D., Wang, L., Sun, B., Shi, P., Wang, L., & Gu, Y. (2020). Microglia mediate forgetting via complement-dependent synaptic elimination. *Science*, 367(6478), 688–694. <https://doi.org/10.1126/science.aaz2288>
- Wolf, C., Rapp, A., Berndt, N., Staroske, W., Schuster, M., Dobrick-Mattheuer, M., Kretschmer, S., König, N., Kurth, T., Wiczorek, D., Kast, K., Cardoso, M. C., Günther, C., & Lee-Kirsch, M. A. (2016). RPA and Rad51 constitute a cell intrinsic mechanism to protect the cytosol from self DNA. *Nature Communications*, 7, 11752. <https://doi.org/10.1038/ncomms11752>
- Yang, X., Diaz, V., & Huang, H. (2022). The role of interferon regulatory factor 1 in regulating microglial activation and retinal inflammation. *International Journal of Molecular Sciences*, 23(23), 14664. <https://doi.org/10.3390/ijms232314664>
- Zhao, K., Du, J., Peng, Y., Li, P., Wang, S., Wang, Y., Hou, J., Kang, J., Zheng, W., Hua, S., & Yu, X. F. (2018). LINE1 contributes to autoimmunity through both RIG-I- and MDA5-mediated RNA sensing pathways. *Journal of Autoimmunity*, 90, 105–115. <https://doi.org/10.1016/j.jaut.2018.02.007>

SUPPORTING INFORMATION

Additional supporting information can be found online in the Supporting Information section at the end of this article.

How to cite this article: Bortolin, V., Mansuroglu, Z., Conquet, L., Calcagno, G., Lambert, F., Marin-Obando, J. P., Segrt, H., Savino, M., Menidjel, R., Souès, S., Buée, L., Niedergang, F., Galas, M.-C., Montagutelli, X., & Bonnefoy, E. (2024). Protein kinase R induced by type I interferons is a main regulator of reactive microglia in Zika virus infection. *Glia*, 1–25. <https://doi.org/10.1002/glia.24619>